Theoretical investigation of iron carbide, FeC

Demeter Tzeli and Aristides Mavridis[a)]
Laboratory of Physical Chemistry, Department of Chemistry, National and Kapodistrian University of Athens, P.O. Box 64 004, 157 10 Zografou, Athens, Greece

(Received 28 September 2001; accepted 21 December 2001)

Employing multireference variational methods (MRCI), we have constructed full potential-energy curves for the ground state ($X\,^3\Delta$) and forty excited states of the diatomic carbide, FeC. For all states we report potential-energy curves, bond lengths, dissociation energies, dipole moments, and certain spectroscopic constants, trying at the same time to get some insight on the bonding mechanisms with the help of Mulliken populations and valence-bond–Lewis diagrams. For the $X\,^3\Delta$ state at the MRCI level of theory, we obtain a dissociation energy $D_e=86.7$ kcal/mol at a bond length $r_e=1.581$ Å. These values compare favorably to the corresponding experimental ones, $D_e=91.2\pm7$ (upper limit) kcal/mol and $r_e=1.5924$ Å. The first excited state ($^1\Delta$) is predicted to be 9.7 kcal/mol above the *X*-state as compared to an experimental value of 9.786 kcal/mol. © *2002 American Institute of Physics.* [DOI: 10.1063/1.1450548]

I. INTRODUCTION

Continuing our effort to rationalize the electronic structure and bonding in the diatomic metal carbide series (neutral or cations) M–C,[1,2] M=first row transition metal element, we report the theoretical investigation of the iron carbide (Fe–C) molecule. In particular, we present high level multireference variational calculations on a total of 41 states, covering an energy range of about 4 eV.

Due to the obvious interest, practical and/or academic in the organometallic bond,[3] diatomic metal carbides constitute interesting, nominally simple systems, which can be thoroughly studied and used as models for the more complex polyatomic organometallic compounds. However, despite their relative simplicity M–C (M=Sc,Ti,V,…) diatomics are not so easily cracked nuts, the reason being the well known complexity inherent in all systems bearing first row transition metal atoms.[4] Perhaps this is the reason why *ab initio* calculations on the M–C series are not abundant.[2,4] Indeed, we are aware of only three *ab initio*[5–7] and one density functional (DFT) study[8] on the FeC molecule.

The Nash *et al.* work[5] deals with the FeC, FeC_2, and FeC_3 carbides at the SCF, MP4, and DFT level of theory. The Shim and Gingerich work[6] involves the examination by multireference variational methods and double zeta quality basis sets of the ground ($X\,^3\Delta$) and a number of low-lying excited states of FeC. Their results will be contrasted with ours in due course. Hirano and co-workers[7] examined the ground ($^3\Delta_{2,3}$) and two excited states, namely, the $^1\Delta$ and $^5\Pi_{1,2}$, employing multireference methods and large basis sets including (scalar) relativistic corrections. We touch upon their results as we move along.

On the experimental side, Balfour *et al.*,[9] using laser-induced fluorescence spectroscopy, determined for the first time that the ground state of the FeC in the gas phase is of $^3\Delta_i$ symmetry, with bond distance(s) $r_0=1.596$ (1.591) Å for the $X\,^3\Delta_3$ ($X\,^3\Delta_2$) state. In addition, two electronic excited states of $\Omega(=|\Lambda+\Sigma|)=3$ symmetry and their relative position with respect to the ground state have been identified.[9]

In 1996 Allen *et al.*,[10] observing for the first time the pure rotational spectrum of FeC, confirmed that the ground state is of $^3\Delta$ symmetry and determined accurately the ground state rotational constant of $^{56}Fe^{12}C$, $B_0''=20\,075.397\,6(66)$ MHz ($=0.669\,643\,18(7)$ cm^{-1}).

Six new electronic states of FeC have been determined and located relative to the ground state by Brugh and Morse[11] by resonant two-photon ionization spectroscopy. Three of these states have $\Omega=3$, one has $\Omega=4$ ($^3\Phi_4$), and two possess $\Omega=2$. Having also obtained the ionization energy (IE) of FeC to be 7.74 ± 0.09 eV, they were able to (indirectly) determine its bond strength (D_0) through the known dissociation energy of FeC^+:[12]

$$\begin{aligned} D_0(\mathrm{FeC}) &= \mathrm{IE(FeC)}+D_0(\mathrm{FeC^+})-\mathrm{IE(Fe)} \\ &= 7.74\pm0.09+4.1\pm0.3^{12}-7.90^{13} \\ &= 3.9\pm0.3\ \mathrm{eV}=90\pm7\ \mathrm{kcal/mol}, \\ &\text{or}\ \ D_e=D_0+\omega_e/2^{14} \\ &= 91.2\pm7\ \mathrm{kcal/mol}. \end{aligned}$$

This is an upper limit value due to the uncertainty in the D_0 value of FeC^+.[12]

More recently, Angeli *et al.*,[15] using threshold photoelectron spectra obtained a D_0 value of FeC^+ of 84.2 ± 4.1 kcal/mol as contrasted to 4.1 ± 0.3 eV$=94.5\pm7$ kcal/mol of Hettich and Freiser.[12] Using the new D_0 (FeC^+) value, one obtains, D_0 (FeC)$=80.5\pm4.6$ kcal/mol, or D_e (FeC)$=D_0+\omega_e/2^{14}=81.7\pm4.6$ kcal/mol.

Aiuchi, Tsuji and Shibuya[14] by dispersed fluorescence spectroscopy observed a new electronic state 3460 cm^{-1} above the $X\,^3\Delta_2$, tentatively assigned to a $^5\Pi_2$ symmetry (but see below).

a)Electronic mail: mavridis@chem.uoa.gr

Finally, Leung and co-workers[16] by laser infrared spectroscopy, they found the spin–orbit splitting between the $X\,^3\Delta_2$ and $X\,^3\Delta_3$ states to be 329.809 cm^{-1}.

We presently report the theoretical examination of 41 states of the FeC diatomic correlating adiabatically to $C(^3P)+Fe(a^5D,a^5F,a^3F,a^3H)$. In particular, the ground-state atoms $C(^3P)+Fe(^5D)$ give rise to 27 states i.e., $^3\Sigma^+[1]$, $^3\Sigma^-[2]$, $^3\Pi[3]$, $^3\Delta[2]$, $^3\Phi[1]$, $^5\Sigma^+[1]$, $^5\Sigma^-[2]$, $^5\Pi[3]$, $^5\Delta[2]$, $^5\Phi[1]$, $^7\Sigma^+[1]$, $^7\Sigma^-[2]$, $^7\Pi[3]$, $^7\Delta[2]$, and $^7\Phi[1]$, all of which but the $^3\Sigma^+[1]$, have been computed. Moreover, three more states were computed, $^3\Delta[2]$ and $^3\Gamma[1]$, correlating to $C(^3P)+Fe(^5F)$. We have also computed eleven out of the twelve singlets, namely, $^1\Sigma^+[1]$, $^1\Sigma^-[1]$, $^1\Pi[3]$, $^1\Delta[3]$, $^1\Phi[2]$, and $^1\Gamma[1]$ correlating to $C(^3P)+Fe(^3F)$, plus one ^1H (*Greek eta*) state correlating to $C(^3P)+Fe(^3H)$ fragments. Numbers in square brackets indicate the number of states in each particular symmetry.

Following the philosophy of our previous work on similar systems,[1,2,17] for all 41 states studied we report potential-energy curves (PEC), total energies (E), binding energies (D_e), bond distances (r_e), dipole moments (μ), spectroscopic parameters and charge distributions. Emphasis has been given in deciphering the bonding process with the help of Mulliken populations and simple valence-bond–Lewis (vbL) diagrams.

In Sec. II we define the technical approach followed; in Sec. III we present some related atomic numerical results, our main body results are discussed in Sec. IV, and some final conclusion and comments are presented in Sec. V.

II. TECHNICAL CONSIDERATIONS

For the Fe atom the ANO basis set of Bauschlicher[18] $(20s15p10d6f4g)$ has been used but without the g functions; for the C atom the correlation consisted basis of triple-z quality of Dunning,[19] cc-pVTZ$=(10s5p2d1f)$ was employed. Both sets were generally contracted to $[(7s6p4d3f)_{Fe}/(4s3p2d1f)_C]$, thus containing 96 spherical Gaussian functions. However, and in order to monitor our results, three out of the 41 examined states, namely the ground $(X\,^3\Delta)$, and the first two excited states $(^1\Delta, ^3\Sigma^-)$, were re-examined using the complete Bauschlicher basis $(+g)$ and the cc-pVQZ for the carbon atom contracted to $[(7s6p4d3f2g)_{Fe}/(5s4p3d2f1g)_C]$, numbering 139 functions (''large basis'').

We are confronted here with an inherently multireference system of 12 ''valence'' (active) electrons; therefore, the only methodology that can cope with such a system, particularly if one wishes to construct full potential-energy curves (PEC) and a multitude of excited states, is a complete active space self consistent field (CASSCF)+configuration interaction (CI) approach, specifically, CASSCF+single +double replacements=MRCI. Twelve valence electrons ($3d^64s^2$ on Fe+$2s^22p^2$ on C) were distributed to 10 orbitals (one $4s$ and five $3d$'s on Fe+one $2s$ and three $2p$'s on C). Depending on the spin multiplicity and the spatial symmetry of the state, our reference space(s) (CAS) ranges from 268 ($^7\Sigma^-$) to 5220 ($^3\Pi$) configuration functions (CF), with corresponding MRCI spaces ranging from 10 218 942 ($^7\Sigma^-$) to 66 339 660 ($^3\Sigma^+$) CFs. By applying the internal contraction (icMRCI) technique,[20] the number of CFs is reduced dramatically ranging from 310 000 to 1 210 000 CFs, thus making the calculations feasible and with tolerable losses in total energies.[17] The corresponding numbers using the large basis set, for the $X\,^3\Delta$ state for instance, are 160 182 461 CFs reduced to about 1 600 000 CFs upon enforcing the icMRCI approach. To estimate core $(3s^23p^6)$ correlation effects, ic-MRCI calculations were performed out of the $12e^-$ CASSCF spaces including the 8 Fe core electrons, with the small and the large basis sets, for the ground $X\,^3\Delta$ state and for the first $(^1\Delta)$ and second $(^3\Sigma^-)$ excited states and for a few points around the equilibrium. These calculations will be referred to as C-MRCI. It is of interest to mention that the number of CFs involved in the C-MRCI (icC-MRCI) computations are 723 362 352 (15 500 000), and 1 757 617 193 (24 340 000) with the small and the large basis sets, respectively for the $X\,^3\Delta$ and $2\,^3\Sigma^-$ states. These numbers rationalize our choice of the basis set, ''small,'' and valence correlation approach for obtaining potential-energy curves for more than 40 FeC states.

All calculations were done under C_{2v} symmetry constraints, nevertheless care was taken for our CASSCF wave functions to posses the correct axial angular momentum symmetry, i.e., $|\Lambda|=0(\Sigma^{\pm})$, 1 ($\Pi$), 2 ($\Delta$), 3 ($\Phi$), 4 ($\Gamma$), and 5 (H). This means that Δ and Γ states are linear combinations of A_1 and A_2 symmetries, Π, Φ, and H states are combinations of B_1 and B_2 symmetries, while Σ^+ and Σ^- states correspond to the A_1 and A_2 symmetry species, respectively. Of course, MRCI wave functions do not display, in general, pure (spatial) angular momentum symmetry, but rather A_1 (or A_2) and B_1 (or B_2). With the exception of the ground, the first and second excited states, the state average (SA) approach[21] was applied for all other states.

Finally, for the $X\,^3\Delta$ state coupled cluster calculations were done, with (C-CCSD(T)) and without (CCSD(T)) the $3s^23p^6$ Fe core electrons. However, we were able to converge these (T) calculations using only CASSCF orbitals to construct the (single) reference function. Lastly, the basis set superposition error (BSSE) was estimated for the ground state by the usual Boys–Bernardi approach.[22]

Due to the relatively large number of active electrons (12), we encountered significant size-nonextensivity problems, 9–10 mh at the MRCI level and for all states; by including the Davidson correction[23] for unlinked clusters (+Q), the nonextensivity error was almost vanished, dropping to an average of 0.3 mh.

All calculations were performed with the MOLPRO 2000 suite of codes.[24]

III. THE Fe AND C ATOMS

Total energies of the Fe ^5D, ^5F, ^3F, and C ^3P terms, and energy splittings $Fe(^3F, ^5F\leftarrow{}^5D)$ at the spherically averaged CASSCF, MRCI, and MRCI+Q levels of theory are presented in Table I along with experimental values.[13] The agreement between theoretical and experimental values cannot be considered as particularly good, the differences being 0.176 and 0.180 eV or 20% and 12%, for the $^5F\leftarrow{}^5D$ and $^3F\leftarrow{}^5D$ separations, respectively (MRCI). Although the

TABLE I. Total energies (Hartree) of the Fe(^5D, ^5F, ^3F) and C(^3P) atoms, and atomic energy separations (eV) of Fe.

Method	Fe ^5D	Fe ^5F	Fe ^3P	$^5F \leftarrow {}^5D$	$^3F \leftarrow {}^5D$	C ^3P
CASSCF[a,b]	−1262.443 14	−1262.357 05	−1262.351 05	2.342	2.506	−37.704 02
MRCI[c,b]	−1262.632 09	−1262.593 47	−1262.570 77	1.051	1.668	−37.779 47
MRCI+Q[b]	−1262.646 8	−1262.612 9	−1262.585 5	0.92	1.67	−37.782 3
CASSCF/large[a,d]	−1262.443 14	−1262.357 05	−1262.351 05	2.342	2.506	−37.705 60
MRCI/large[c,d]	−1262.642 44	−1262.605 94	−1262.583 77	0.993	1.597	−37.784 93
MRCI+Q/large[d]	−1262.657 8	−1262.625 9	−1262.599 3	0.87	1.59	−37.787 9
Expt.[e]				0.875	1.488	

[a]Spherically averaged CASSCF with 5 determinants (^5D), 7 determinants (^5F, ^3F), 3 determinants (^3P).
[b]Basis set [$7s6p4d3f/_{\mathrm{Fe}}$ cc-pVTZ/$_{\mathrm{C}}$].
[c]Internally contracted MRCI.
[d]Basis set [$7s6p4d3f2g/_{\mathrm{Fe}}$ cc-pVQZ/$_{\mathrm{C}}$].
[e]Reference 13.

Davidson correction improves significantly, the former leaves the latter intact.

IV. RESULTS AND DISCUSSIONS

Table II gives total energies (E), equilibrium distances (r_e), dissociation energies (D_e) with respect to the adiabatic products, dipole moments (μ), Mulliken charges (q), harmonic frequencies and anharmonic corrections ($\omega_e, \omega_e x_e$), rotational vibrational couplings (α_e), centrifugal distortions ($\bar{D}_e$), and energy gaps (T_e) at the CASSCF, icMRCI, and icMRCI+Q level of theory, of forty one states with spatial-spin symmetries $^{1,3,5,7}\Sigma^{\pm}$, $^{1,3,5,7}\Pi$, $^{1,3,5,7}\Delta$, $^{1,3,5,7}\Phi$, $^{1,3}\Gamma$ and ^{1}H. Subscripts G and L refer to global and local minima, respectively. Figure 1 shows relative energies of all states studied covering an energy range of 3.7 eV, while Fig. 2 presents the totality of PECs. Each excited state has been labeled with a serial number in front of the symmetry symbol revealing its absolute energy order with respect to the ground (X) state, and a number in parentheses indicating its absolute order within the same space–spin symmetry manifold. Figures 3–10 present separately the PECs, according to their spin multiplicity.

In the ensuing discussion we analyze first the triplets followed by the quintets, and then the septets; 26 of these states correlate to the ground-state atoms, Fe(^3D)+C(^3P), while three states correlate to the first excited state of Fe, $^5F(d^7s^1)$. Then we discuss the 11 singlets correlating to the second excited state of Fe(^3F)(+C(^3P)), and finally one ^{1}H state correlating to the sixth excited state of Fe(^3H)(+C(^3P)).

A. Triplets: $X\,^3\Delta$, $2\,^3\Sigma^-(1)$, $5\,^3\Pi(1)$, $7\,^3\Delta(2)$, $8\,^3\Pi(2)$, $16\,^3\Sigma^-(2)$, $18\,^3\Phi(1)$, $20\,^3\Pi(3)$, $29\,^3\Delta(3)$, $33\,^3\Delta(4)$, and $34\,^3\Gamma(1)$

$$X\,^3\Delta(\sim 0.81|(1/\sqrt{2})(1\sigma^2 2\sigma^2 3\sigma^1 1\pi_x^2 1\pi_y^2) \times (1\delta_+^2 1\delta_-^1 + 1\delta_+^1 1\delta_-^2)\rangle = |A_1\rangle + |A_2\rangle, \mathrm{CASSCF}).$$

Notice that our orbital notation refers only to the 12 valence electrons, i.e., we do not number the doubly occupied six σ and four π "core" orbitals; $|A_1\rangle+|A_2\rangle$ gives the spatial symmetry of the wave functions in C_{2v}, and the acronym "CASSCF" (or "MRCI") refers to the origin of the leading variational coefficient(s), 0.81 in the present case in the CASSCF wave function.

In agreement with the experimental results[9–11,14] and recent *ab initio* calculations,[6,7] the ground state of FeC is of $^3\Delta$ symmetry. As we can see from Table II moving from the MRCI, to C-MRCI, to MRCI/large, and to C-MRCI/large, the $X\,^3\Delta$ D_e value increases steadily, to a final value of 86.7 kcal/mol. Taking into account the BSSE correction (−0.4 kcal/mol) and scalar relativistic effects[6] (−2 kcal/mol), our best estimate is $D_e = 84.3$ kcal/mol, within the range of experimental values, 91.2 ± 7 kcal/mol (upper limit),[11] and 81.7 ± 4.6 kcal/mol.[15] Similarly our best C-MRCI/large basis $r_e = 1.581$ Å, is in respectable agreement with the experimental value(s). Notice the shortening of r_e by about 0.01 Å when the Fe $3s^2 3p^6$ core electrons are included in the MRCI calculation.

At infinity the wave function can be described by the product $|^5D; M=\pm 2\rangle_{\mathrm{Fe}} \times |^3P; M=0\rangle_{\mathrm{C}}$. As the two atoms come together, Fig. 3, and around 4.5 bohr, the $X^3\Delta$ state suffers an avoided crossing with the $7^3\Delta(2)$ state which correlates *diabatically* to Fe(^5F)+C(^3P). As a result the *in situ* equilibrium atoms are of Fe(^5F; M=±2)+C(^3P; M=0) character, and the bonding can be described pictorially by the following valence–bond–Lewis (vbL) icons

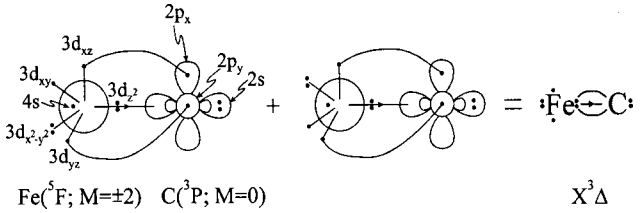

The above bonding diagram is in agreement with CASSCF Mulliken equilibrium atomic populations (Fe/C),

$$4s^{0.84} 4p_z^{0.22} 3d_{z^2}^{1.21} 3d_{xz}^{1.18} 4p_x^{0.03} 3d_{yz}^{1.18} 4p_y^{0.03} (3d_{x^2-y^2} 3d_{xy})^{3.00} / 2s^{1.82} 2p_z^{0.87} 2p_x^{0.78} 2p_y^{0.78}.$$

Clearly we have two π bonds ($1.18+0.03+0.78=1.99$ e$^-$) $\times 2$ and one σ, the latter caused by the transfer of 0.7 e$^-$ from the Fe $3d_z2$ to the $2p_z$ orbital of the C atom. The extra ~ 0.2 e$^-$ of C $2p_z$ are pumped from the $2s$ orbital. The final result is a genuine triple bond, with a total transfer of 0.29

TABLE II. Absolute energies E (Hartree), bond lengths r_e (Å), binding energies D_e (kcal/mol), harmonic frequencies and anharmonic correction ω_e, $\omega_e x_e$ (cm^{-1}), rotational vibrational couplings α_e (cm^{-1}), centrifugal distortions $\overline{D}_e$(cm^{-1}), Mulliken charges on C q_C, dipole moments μ (Debye) and energy differences T_e (kcal/mol), at CASSCF, MRCI,[a] and MRCI+Q[b] level. Experimental and other theoretical results are also included.

State[c]	Methods	$-E$	r_e	D_e	ω_e	$\omega_e x_e$	$\alpha_e(10^{-3})$	$\overline{D}_e(10^{-7})$	$-q_C$	μ	T_e
$X\ ^3\Delta$	CASSCF	1300.233 82	1.640	53.7(53.7°)	622	43			0.29	1.48	0.0
	MRCI	1300.528 03	1.605	79.6(78.7°)	810.1	7.71	8.02	17.7	0.23	1.34	0.0
	MRCI+Q	1300.554 0	1.609	80.4(79.5°)							0.0
	CCSD(T)	1300.551 68	1.583	76.1	892						
	C-MRCI[d]	1300.813 66	1.596	81.3	834				0.24	1.28	
	C-MRCI+Q[d]	1300.870 7	1.598	84.2							
	C-CCSD(T)[d]	1300.881 08	1.569	76.7	958						
	CASSCF/large[e]	1300.236 38	1.635	54.2(54.2°)	631.4	40.9	21.9	26.2	0.21	1.49	
	MRCI/large[e]	1300.549 54	1.593	83.5(83.1°)	840.8	7.34	7.61	17.2	0.13	1.34	
	MRCI+Q/large[e]	1300.577 1	1.596	84.7(84.2°)							
	C-MRCI/large[d,e]	1300.881 41	1.581	86.7	877				0.13	1.25	
	C-MRCI+Q/large[d,e]	1300.945 0	1.582	90.5							
	MP4/SCF[f]		1.92	95.5							
	DFT/LDA[f]		1.54	143.2							
	DFT/NL[f]		1.57	107.0							
	DFT/LDA[g]		1.565	155.6							
	MRCI[h]		1.589	66.4	848					1.855	
	MRCI+rel[h,i]		1.585	64.3	859	−4.5					
	MRCI+Q[j]		1.5931	81.9	866.0	8.7	8	16.2		1.30	
	MRCI+Q+rel[j,i,k]		1.5907	81.2	871.5	9.0	8	16.1		1.29	
	MRCI+Q+rel[j,i,l]		1.5912	80.0	868.8	9.0	8	16.2		1.29	
	Expt.[k]		1.596[m]	91.2±7[p,q]	862.9±6.2[s]	7.5±0.8[s]					
	Expt.[k]		1.59621[n]	81.7±4.6[r]	~804[t]						
	Expt.[l]		1.591[m]		866.6±8.2[s]	8.3±1.5[s]					
	Expt.[l]		1.592 39[n]								
$1\ ^1\Delta(1)$	CASSCF	1300.217 80	1.607	99.0	786.9	13.4	10.1	18.7	0.23	1.00	10.0
	MRCI	1300.512 47	1.585	107.4	881.5	6.34	6.77	16.1	0.18	0.94	9.8
	MRCI+Q	1300.539 0	1.590	109							9.4
	CASSCF/large[e]	1300.220 49	1.603	99.6	792.4	13.5	1.01	1.87	0.13	1.01	10.0
	MRCI/large[e]	1300.534 43	1.575	110.0	906.8	6.37	6.51	1.58	0.07	0.92	9.5
	MRCI+Q/large[e]	1300.562 5	1.578	112							9.1
	C-MRCI/large[d,e]	1300.865 97	1.566	111.0	954				0.07	0.80	9.7
	C-MRCI+Q/large[d,e]	1300.929 9	1.567	114							9.5
	MRCI[h]		1.572		933					1.51	9.88
	MRCI+rel[h,i]		1.567		962	−16.2					10.63
	MRCI+Q[j]		1.5778		907.4	6.3	6	15.6		0.87	9.22
	MRCI+Q+rel[j,i]		1.5733		922.8	6.5	6	15.4		0.85	10.01
	Expt.		1.595[m]								10.74[u]
	Expt.[s]		1.5739		938±21	8.9±5.0					9.786
$2\ ^3\Sigma^-(1)$	CASSCF	1300.211 25	1.735	39.0	555.4	41.9	21.7	23.6	0.27	1.10	14.2
	MRCI	1300.511 64	1.694	69.1	788.9	−0.1	2.90	13.5	0.20	1.16	10.3
	MRCI+Q	1300.543 1	1.693	74							6.9
	CASSCF/large[e]	1300.213 09	1.731	39.4	564.2	43.4	21.4	23.4	0.23	1.10	14.6
	MRCI/large[e]	1300.530 90	1.686	71.7	798.2	−1.7	3.15	13.6	0.16	1.17	11.7
	MRCI+Q/large[e]	1300.563 8	1.684	76							8.3
	C-MRCI/large[d,e]	1300.858 81	1.675	72.4	835				0.15	1.00	14.1
	C-MRCI+Q/large[d,e]	1300.927 7	1.670	80							10.8
	MRCI[h]		1.688		722					1.948	15.2
	MRCI+rel[h,i]		1.672		761	0.3					10.98
$3\ ^5\Pi(1)$	CASSCF	1300.196 07	2.002	30.2					0.45	2.66	23.7
	MRCI	1300.488 14	1.689	54.6	707.1	1.61	−1.75	16.9	0.33	2.44	25.1
	MRCI+Q	1300.520 1	1.656	59.2							21.2
	DFT/LDA[g]		1.628	138							17.6
	MRCI[h]		1.643		823					2.773	32.0
	MRCI+rel[h,i]		1.637		848	−27.4					31.1
	MRCI+Q[j]		1.6514		830.9	4.5	5	14.2		2.42	21.5
	MRCI+Q+rel[j,i,v]		1.6459		852.4	4.8	5	13.7		2.41	20.6
	MRCI+Q+rel[j,i,w]		1.6466		850.0	4.8	5	13.8		2.42	20.7
$4\ ^5\Delta(1)$	CASSCF	1300.211 01	2.009	39.7					0.45	2.36	14.3

TABLE II. (*Continued*.)

State[c]	Methods	$-E$	r_e	D_e	ω_e	$\omega_e x_e$	$\alpha_e(10^{-3})$	$\overline{D}_e(10^{-7})$	$-q_C$	μ	T_e
	MRCI	1300.482 85	1.884	51.3	552.7	1.73	3.65	14.5	0.36	1.67	28.3
	MRCI+Q	1300.508 2	1.861	51.6							28.7
	MRCI[h]		1.900		559					1.732	22.5
	MRCI+rel[h,i]		1.897		562	−5.2					22.5
$5\,^3\Pi(1)$	CASSCF	1300.192 99	2.045	28.3					0.49	3.42	25.6
	MRCI	1300.473 08	1.854	45.1	510.4	1.97	4.75	18.8	0.37	2.62	34.5
	MRCI+Q	1300.502 3	1.814	47.9							32.5
	MRCI[h]		1.933		373					3.245	44.3
	MRCI+rel[h,i]		1.937		384	5					43.8
$6\,^5\Sigma^-(1)$	CASSCF	1300.192 10	2.025	28.0					0.44	2.36	26.2
	MRCI	1300.471 05	1.883	43.9	552.7	4.44	3.14	14.6	0.33	1.71	35.8
	MRCI+Q	1300.500 6	1.864	46.9							33.5
	MRCI[h]		1.911		555					2.116	23.5
$7\,^3\Delta(2)$	CASSCF	1300.187	2.0	25							29
	MRCI	1300.467 85	1.791	42.0	716	8			0.27	1.38	37.8
	MRCI+Q	1300.496 0	1.776	43.9							36.4
	MRCI[h]		1.860		833					1.952	40.0
	Expt.[k,m]		1.713								
	Expt.[l,m]		1.693								
	Expt.[p]		1.752 64(26)		732(2)	4.1(2)	4.489				37.84
$8\,^3\Pi(2)$	CASSCF	1300.162 60	1.906	9.06					0.42	2.80	44.7
	MRCI	1300.461 34	1.684	37.8	948.2	62.0	13.6	9.73	0.31	2.50	41.8
	MRCI+Q	1300.493 0	1.676	41.9							38.3
	Expt.[x,y]		1.621 45(12)[p]		910.8[p]	14.9[p]					37.28[p,u]
	Expt.[z,y]										37.6[u]
$9\,^7\Delta(1)$	CASSCF	1300.199 13	2.084	32.3					0.47	2.42	21.8
	MRCI	1300.460 79	2.035	37.4	546.8	5.31	5.16	9.51	0.41	2.13	42.2
	MRCI+Q	1300.483 8	2.035	36.3							44.1
	MRCI[h]		2.036		557					2.417	19.2
$10\,^7\Pi(1)$	CASSCF	1300.186 82	2.091	24.4					0.48	2.67	29.5
	MRCI	1300.453 64	2.006	32.9	437.5	6.63	1.25	13.7	0.41	2.39	46.7
	MRCI+Q	1300.478 5	1.991	33.0							47.4
	MRCI[h]		1.997		481					2.799	33.6
$11\,^1\Pi(1)$	CASSCF	1300.162 95	1.918	67.1					0.41	2.11	44.5
	MRCI	1300.452 87	1.741	70.9	692.6	8.43	5.83	14.8	0.27	1.64	47.2
	MRCI+Q	1300.483 8	1.717	74.4							44.1
	MRCI[h]		1.718		704					2.302	58.3
$12\,^5\Sigma^-(2)$	CASSCF	1300.159 78	1.925	7.9					0.42	2.04	46.5
	MRCI	1300.451 97	1.802	32.0	782.7	0.75	3.98	9.44	0.30	1.41	47.7
	MRCI+Q	1300.482 8	1.784	35.7							44.7
$13\,^7\Sigma^-(1)$	CASSCF	1300.182 49	2.103	21.9					0.47	2.60	32.2
	MRCI	1300.449 04	2.040	30.1	489.3	3.03	3.21	11.5	0.40	2.31	49.6
	MRCI+Q	1300.474 8	2.032	30.7							49.7
	MRCI[h]		2.053		502					2.858	36.3
$14\,^1\Gamma(1)$	CASSCF	1300.146 25	1.643	56.6					0.23	0.91	54.9
	MRCI	1300.445 00	1.641	66.1	898.0	4.66	4.56	12.7	0.18	0.96	52.1
	MRCI+Q	1300.475 7	1.643	69.5							49.1
$15\,^5\Delta(2)$	CASSCF	1300.171 55	2.027	15.5					0.43	2.14	39.1
	MRCI	1300.443 53	1.952	26.8	629.0	36.0	3.58	9.07	0.34	1.79	53.0
	MRCI+Q	1300.469 0	1.942	27.0							53.3
$16\,^3\Sigma^-(2)$	CASSCF	1300.153 94	1.834	4.2					0.39	1.43	50.1
	MRCI	1300.442 43	1.799	26.0	663				0.27	0.61	53.7
	MRCI+Q	1300.473 3	1.766	29.7							50.6
$17\,^5\Pi(2)$	CASSCF	1300.158 96	2.003	7.3					0.42	2.23	47.0
	MRCI	1300.439 87	1.806	24.3	703	71.5	1.12	10.3	0.31	1.72	55.3
	MRCI+Q	1300.469 1	1.781	27.0							53.3
$18\,^3\Phi(1)$	CASSCF	1300.134 95	1.897	−8.1					0.25	1.80	62.0
	MRCI	1300.439 36	1.795	23.9	675.5	6.51	5.62	13.0	0.18	1.46	55.7
	MRCI+Q	1300.472 4	1.791	29.1							51.2
$19\,^1\Sigma^+(1)$	CASSCF	1300.129 09	1.681	45.8					0.26	1.53	65.7

TABLE II. (*Continued*.)

State[c]	Methods	$-E$	r_e	D_e	ω_e	$\omega_e x_e$	$\alpha_e(10^{-3})$	$\overline{D}_e(10^{-7})$	$-q_C$	μ	T_e
	MRCI	1300.438 48	1.660	61.8	863.2	3.99	4.30	12.8	0.21	1.51	56.2
	MRCI+Q	1300.471 3	1.658	66.6							51.9
$20\,^3\Pi(3)$	CASSCF	1300.132 40	1.952	−8.5					0.26	1.93	63.6
	MRCI	1300.435 61	1.813	22.1	650.4	6.75	5.58	13.2	0.19	1.53	58.0
	MRCI+Q	1300.468 7	1.808	27.0							53.5
$21\,^1\Sigma^-(1)$	CASSCF	1300.150 29	2.005	59.8					0.44	1.95	52.4
	MRCI	1300.432 79	1.817	58.6	567.0	4.03	14.0	17.1	0.27	0.43	59.8
	MRCI+Q	1300.465 3	1.767	62.9							55.6
$22\,^7\Delta(2)$	CASSCF	1300.167 05	2.113	12.7					0.46	2.49	41.9
	MRCI	1300.430 97	2.081	18.9	565.5	2.95	3.62	7.67	0.39	2.29	60.9
	MRCI+Q	1300.454 7	2.08	18.0							62.3
$23\,^5\Sigma^+(1)$	CASSCF	1300.138 54	2.021	−5.7					0.45	2.75	59.8
	MRCI	1300.428 68	1.854	17.3	567.4	10.4	6.40	15.2	0.35	1.99	62.3
	MRCI+Q	1300.460 2	1.829	21.5							58.8
$24\,^5\Pi_G(3)$	CASSCF	1300.145 17	2.162	−0.5					0.40	2.91	55.6
	MRCI	1300.427 94	1.946	17.2	658.3	48.8	9.50	7.97	0.39	2.51	62.8
	MRCI+Q	1300.457 3	1.950	19.8							60.7
$24\,^5\Pi_L(3)$	CASSCF	1300.143 12	1.954	−1.8					0.45	2.78	56.9
	MRCI	1300.420 8	1.69	13					0.34	2.04	67
	MRCI+Q	1300.453 5	1.68	17							63
$25\,^7\Pi(2)$	CASSCF	1300.157 66	2.090	6.5					0.46	2.39	47.8
	MRCI	1300.427 11	2.019	16.3	567.1	13.9	4.32	9.13	0.37	2.02	63.4
	MRCI+Q	1300.452 5	2.009	16.5							63.7
$26\,^5\Phi(1)_G$	CASSCF	1300.117 53	1.699	−19.0					0.38	2.34	73.0
	MRCI	1300.426 78	1.695	16.0	1240				0.33	2.23	63.5
	MRCI+Q	1300.460 7	1.693	21.7							58.5
$26\,^5\Phi(1)_L$	CASSCF	1300.145 88	2.153	−1.3					0.40	2.86	55.2
	MRCI	1300.422 20	2.031	13.1	466				0.31	1.84	66.4
	MRCI+Q	1300.448 7	2.007	14.2							66.1
$27\,^7\Sigma^+(1)$	CASSCF	1300.121 82	1.865	−16.2					0.47	2.34	70.3
	MRCI	1300.425 88	1.766	15.5	766.8	13.5	9.14	10.1	0.37	2.31	64.1
	MRCI+Q	1300.461 1	1.758	22.1							58.3
$28\,^7\Sigma^-(2)$	CASSCF	1300.155 06	2.100	4.9					0.47	2.51	49.4
	MRCI	1300.424 00	2.023	14.5	570.2	3.47	3.85	8.92	0.39	2.04	65.3
	MRCI+Q	1300.450 2	2.006	15.2							65.2
$29\,^3\Delta(3)$	CASSCF	1300.116 06	1.837	21.5					0.34	1.73	73.9
	MRCI	1300.416 88	1.780	33.7	812	53			0.26	1.35	69.7
	MRCI+Q	1300.448 2	1.78	38.6							66.4
$30\,^7\Pi(3)_G$	MRCI	1300.415 19	1.850	9.25	881				0.32	1.75	70.8
	MRCI+Q	1300.446 5	1.865	13.1							67.5
$30\,^7\Pi(3)_L$	CASSCF	1300.143 30	2.230	−1.7					0.40	2.97	56.8
	MRCI	1300.414 38	2.186	8.74	444.7	2.70	3.47	9.19	0.34	2.35	71.4
	MRCI+Q	1300.439 6	2.192	8.8							71.8
$31\,^7\Phi(1)$	CASSCF	1300.143 27	2.230	−2.9					0.40	2.97	56.8
	MRCI	1300.414 35	2.184	8.20	440.2	3.35	3.17	9.46	0.34	2.35	71.4
	MRCI+Q	1300.439 5	2.191	8.4							71.8
$32\,^1\Delta(2)$	CASSCF	1300.109 69	1.798	33.7					0.30	1.43	77.9
	MRCI	1300.412 40	1.740	45.8	820.0	3.43	3.34	10.6	0.24	1.14	72.6
	MRCI+Q	1300.444 1	1.729	49.6							68.9
	Expt[m]		1.740								
$33\,^3\Delta(4)$	CASSCF	1300.107 26	1.809	16.6					0.38	2.17	79.4
	MRCI	1300.407 24	1.774	28.0	808	−9.0			0.29	1.81	75.8
	MRCI+Q	1300.438 8	1.753	32.9							72.3
$34\,^3\Gamma(1)$	CASSCF	1300.103 99	1.837	13.9					0.38	2.14	81.5
	MRCI	1300.403 76	1.798	25.5					0.29	1.74	78.0
	MRCI+Q	1300.434 4	1.793	30.1							75.0
$35\,^1H(1)$	CASSCF	1300.107 58	1.809	35					0.40	2.19	79.2
	MRCI	1300.401 51	1.685	62.4	751.3	8.08	5.59	15.4	0.29	1.81	79.4
	MRCI+Q	1300.429 6	1.680	65							78.1
$36\,^1\Pi(2)$	CASSCF	1300.104 02	1.960	31.4					0.42	2.35	81.4
	MRCI	1300.399 86	1.711	38.0	730.2	2.70	1.85	14.8	0.27	1.45	80.4

TABLE II. (*Continued.*)

State[c]	Methods	$-E$	r_e	D_e	ω_e	$\omega_e x_e$	$\alpha_e(10^{-3})$	$\bar{D}_e(10^{-7})$	$-q_C$	μ	T_e
	MRCI+Q	1300.430 5	1.704	41.0							77.5
$37\,^1\Phi(1)_G$	CASSCF	1300.105 92	1.957	31.3					0.42	2.29	80.3
	MRCI	1300.396 72	1.756	35.7	1011				0.25	1.60	82.4
	MRCI+Q	1300.428 5	1.745	39.7							78.8
$37\,^1\Phi(1)_L$	MRCI	1300.395 83	1.694	35.1	691				0.29	1.7	83.0
$38\,^1\Phi(2)$	CASSCF	1300.095 56	1.863	25.8					0.36	2.01	86.8
	MRCI	1300.395 68	1.724	35.5					0.29	1.7	83.1
	MRCI+Q	1300.425 1	1.706	37.8							80.9
$39\,^1\Pi(3)$	CASSCF	1300.092 91	1.965	24.4					0.41	2.32	88.4
	MRCI	1300.392 92	1.731	33.6	810.3	6.97	6.65	11.2	0.26	1.59	84.8
	MRCI+Q	1300.424 8	1.713	37.5							81.1
$40\,^1\Delta(3)$	CASSCF	1300.100 5	1.88	28					0.41	2.2	84
	MRCI	1300.388 10	1.820	30.6	630.3	13.7	5.82	13.7	0.32	1.63	87.8
	MRCI+Q	1300.417 9	1.790	33.2							85.4

[a]Internally contracted MRCI.
[b]+Q refers to the multireference Davidson correction.
[c]The numbers in parentheses refer to the ordering of states according to energy within the same symmetry manifold.
[d]Core $3s^2 3p^6$ of Fe atom included at the MRCI.
[e]Large basis set, $[7s6p4d3f2g]_{Fe}$/cc-pVQZ/$_C$.
[f]Reference 5, MP4 (or DFT), no specification of the state.
[g]Reference 8; it is only reported that the ground state is a triplet, the spatial angular momentum is not specified.
[h]Reference 6, MRCI/$[8s6p3d1f/_{Fe}4s3p1d/_C]$.
[i]Scalar relativistic corrections included.
[j]Reference 7, MRCI+Q/$[8s7p5d3f2g/_{Fe}$aug-cc-pVQZ/$_c]$.
[k] $^3\Delta_3$.
[l] $^3\Delta_2$.
[m]Reference 9.
[n]Reference 10.
[o]D_e values corrected for BSSE.
[p]Reference 11.
[q]The D_e value has been extracted using the $D_0(FeC^+)$ value of Ref. 12.
[r]The D_e value has been extracted using the $D_0(FeC^+)$ value of Ref. 15.
[s]Reference 14.
[t] $\Delta G_{1/2}$, $\Delta G_{1/2} \cong \omega_e - 2\omega_e x_e$.
[u]Reference 17.
[v] $^5\Pi_1$.
[w] $^5\Pi_2$.
[x] $^3\Phi_4$.
[y]Our results suggest that this experimentally assigned $^3\Phi(1)$ state could be the $^3\Pi(2)$ state.
[z] $^3\Phi_3$.

(0.23) e^- at the CASSCF (MRCI) level from Fe to C. Due to the avoided crossing previously mentioned, *diabatically*, the $X\,^3\Delta$ state correlates to $Fe(^5F)+C(^3P)$, therefore, with respect to these products, i.e., the internal bond strength is, $86.7+\Delta E(^5F \leftarrow {}^5D)=109.6$ kcal/mol (Table I) at the C-MRCI/large level. Clearly, and for obvious reasons, the $3d_{x^2-y^2}$ (δ_+) and $3d_{xy}$ (δ_-) are nonbonding observer electrons and the same holds for all states studied.

$$2\,^3\Sigma^-(1)(\sim|1\sigma^2 2\sigma^2 3\sigma^1[0.71(1\pi_x^2 1\pi_y^2) + 0.20(1\pi_x^2 1\bar{\pi}_y^1 2\pi_y^1) + 0.20(1\bar{\pi}_x^1 2\pi_x^1 1\pi_y^2) - 0.17(1\pi_x^2 2\pi_y^2) - 0.17(2\pi_x^2 1\pi_y^2)]1\delta_+^1 1\delta_-^1\rangle = |A_2\rangle, \text{MRCI}).$$

We believe that this is the *second* excited state 10.3(6.9), or 14.1(10.8) kcal/mol above the X state at the MRCI(+Q) levels of theory, respectively, competing with the $^1\Delta$ state whose corresponding energy distance(s) from the X state is 9.8(9.4), or 9.7(9.5) kcal/mol (*vide infra*), Table II, Figs. 1 and 3. With the exception of μ our results are in relative agreement with those of Shim and Gingerich (SG).[6] At infinity we start with the product wave function $|^5D;M=0\rangle_{Fe} \times |^3P;M=0\rangle_C$, the character of which seems to be maintained along the internuclear distance despite its interaction with the $16\,^3\Sigma^-(2)$ around 5.7 bohr. The strong multireference character of this state does not allow for a simple bonding description; we rather have two π and one σ bond, the latter caused by a transfer of 0.8 e^- to the C $2p_z$ orbital from a $(4s4p_z3d_{z^2})^{4.0}$ hybrid on Fe, in accordance to the CASSCF population analysis (Fe/C)

$$4s^{1.24}4p_z^{0.24}3d_{z^2}^{1.62}3d_{xz}^{1.28}4p_x^{0.03}3d_{yz}^{1.28}4p_y^{0.03}3d_{x^2-y^2}^{1.00}3d_{xy}^{1.00}/ 2s^{1.82}2p_z^{1.05}2p_x^{0.68}2p_y^{0.68}.$$

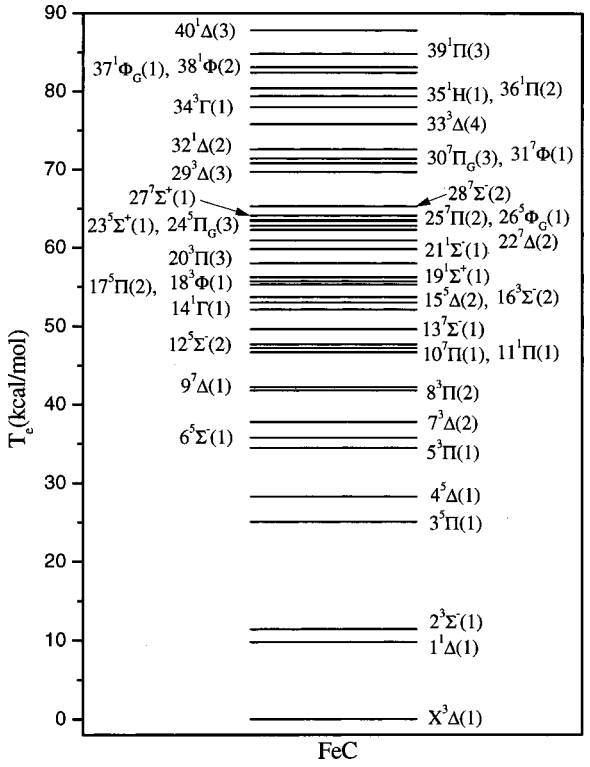

FIG. 1. Relative energy levels of the FeC at the MRCI/$[7s6p4d3f/_{\mathrm{Fe}}$ cc-pVTZ/$_{\mathrm{C}}]$ level.

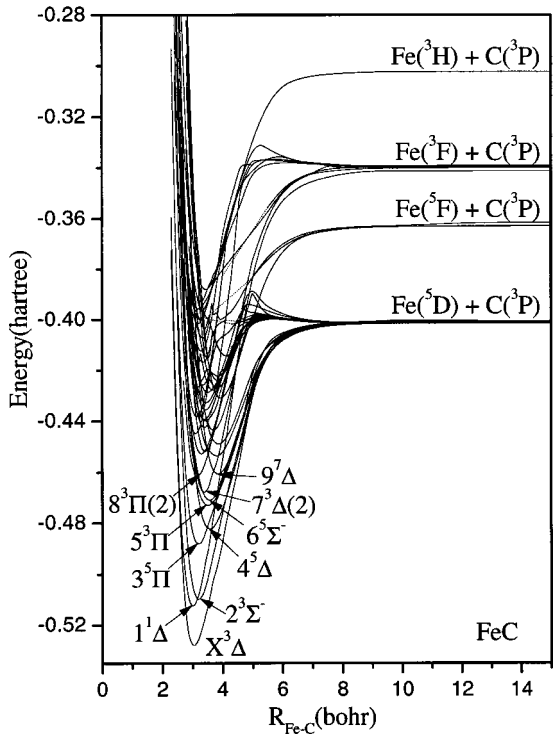

FIG. 2. Potential-energy curves of the 41 states of FeC system at the MRCI/$[7s6p4d3f/_{\mathrm{Fe}}$ cc-pVTZ/$_{\mathrm{C}}]$ level of theory.

$$5\,^3\Pi(1)(\sim|1\sigma^2 2\sigma^2 3\sigma^1 1\delta_+^1[0.42(1\pi_x^2 1\pi_y^2 2\overline{\pi}_y^1)$$
$$+0.41(1\pi_x^1 2\overline{\pi}_x^1 1\pi_y^2 2\overline{\pi}_y^1)-0.19(2\pi_x^2 1\pi_y^2 2\overline{\pi}_y^1)]1\delta_-^1\rangle$$
$$+|1\sigma^2 2\sigma^1 3\overline{\sigma}^1 4\sigma^1 1\delta_+^1[0.25(1\pi_x^2 1\pi_y^2 2\overline{\pi}_y^1)$$
$$+0.32(1\pi_x^1 2\overline{\pi}_x^1 1\pi_y^2 2\overline{\pi}_y^1)]1\delta_-^1\rangle=|B_1\rangle,\mathrm{CASSCF}).$$

This is the lowest state of the $^3\Pi$ manifold 34.5 kcal/mol above the X state, Table II. Our results are at variance from the results of SG.[6] The PEC shown in Fig. 4 shows that it correlates to Fe $(^5D;\mathrm{M}=\pm1)+\mathrm{C}(^3P;\mathrm{M}=0)$, maintaining this character up to the equilibrium (3.5 bohr). However, there is an avoided crossing at 3.05 bohr (repulsive branch) with the $8\,^3\Pi(2)$ state. Practically, the bonding can be described as $\sigma^2\pi^2$, with the σ bond originating from a $(4s4p_z)^{1.92}$ hybrid on Fe and 0.65 e^- migrating from this hybrid to the $2p_z$ C orbital, as indicated by the CASSCF (B_1 symmetry) equilibrium atomic distributions,

$$4s^{1.03}4p_z^{0.24}3d_{z^2}^{1.07}3d_{xz}^{1.08}4p_x^{0.04}3d_{yz}^{2.00}4p_y^{0.04}3d_{x^2-y^2}^{1.00}3d_{xy}^{1.00}/$$
$$2s^{1.82}2p_z^{0.83}2p_x^{0.88}2p_y^{0.94}.$$

A total transfer of 0.5 (0.37) e^- is observed from Fe to C at the CASSCF (MRCI) level.

$$7\,^3\Delta(2)(\sim|[0.38(1\sigma^2 2\sigma^1 3\sigma^2)-0.24(1\sigma^2 2\sigma^1 3\overline{\sigma}^1 4\sigma^1)$$
$$-0.18(1\sigma^2 2\sigma^2 3\sigma^1)](1\pi_x^2 1\pi_y^2 1\delta_+^1 1\delta_-^1)\rangle$$
$$+0.28|1\sigma^2 2\sigma^2 3\sigma^1(1\overline{\pi}_x^1 2\pi_x^1 1\pi_y^2$$
$$+1\pi_x^2 1\overline{\pi}_y^1 2\pi_y^1)1\delta_+^2 1\delta_-^1\rangle=|A_2\rangle,\mathrm{MRCI}).$$

Table II reveals excellent agreement between theory and experiment[11] in the T_e value at the MRCI level, however, we predict an equilibrium distance 0.04 Å larger than the experimental one. Figure 3 depicts the $7\,^3\Delta(2)$ PEC with

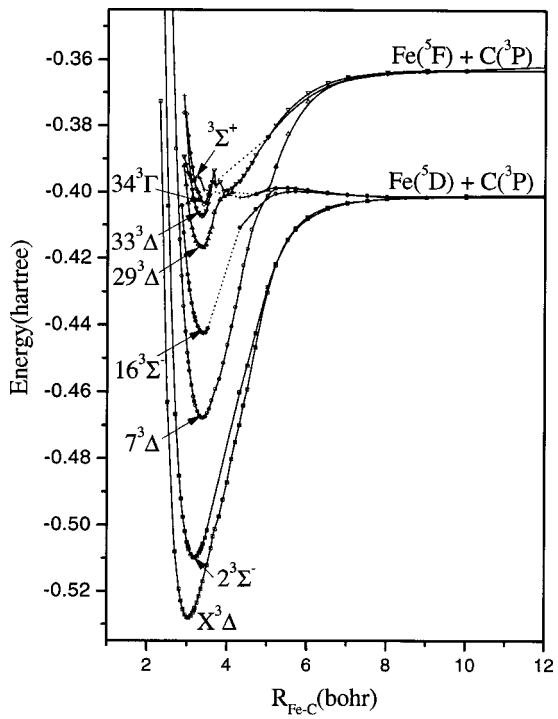

FIG. 3. MRCI potential-energy curves of the triplets $X\,^3\Delta$, $2\,^3\Sigma^-(1)$, $7\,^3\Delta(2)$, $16\,^3\Sigma^-(2)$, $29\,^3\Delta(3)$, $33\,^3\Delta(4)$, $34\,^3\Gamma(1)$, and $^3\Sigma^+(1)$ of the FeC molecule. Dotted lines are referred to those parts of the $16\,^3\Sigma^-(2)$, $29\,^3\Delta(3)$, $34\,^3\Gamma(1)$, and $^3\Sigma^+(1)$ states that have not been calculated.

asymptotic fragments $Fe(^5D;M=\pm1)+C(^3P;M=\pm1)$. Moving towards equilibrium the $^3\Delta(2)$ state suffers an avoided crossing around 5 bohr with the $29\,^3\Delta(3)$ state; a second avoided crossing occurs at ~4.5 bohr with the $X\,^3\Delta$. As a result the *in situ* equilibrium atoms find themselves in $Fe(^5D;M=\pm2)+C(^3P;M=0)$. The equilibrium Mulliken MRCI distributions are

$$4s^{1.01}4p_z^{0.24}3d_{z^2}^{1.15}3d_{xz}^{1.11}4p_x^{0.05}3d_{yz}^{1.11}4p_y^{0.05}3d_{x^2-y^2}^{1.98}3d_{xy}^{1.00}/2s^{1.71}2p_z^{0.85}2p_x^{0.84}2p_y^{0.84},$$

suggesting two π bonds and one σ bond between a $4s4p_z3d_z2$ hybrid on Fe and the empty $2p_z$ of the carbon atom. Alternatively, we can say that about 0.6 e^- are transferred from the Fe $4s$ to the C $2p_z$ orbital, while 0.4 e^- (0.24+0.15) are promoted from the $4s$ to the $4p_z$ and $3d_z2$ atomic functions.

$$8\,^3\Pi(2)(\sim|[0.61(1\sigma^2 2\sigma^2 3\sigma^1 1\bar{\delta}^1_+)+0.19(1\sigma^2 2\sigma^1 3\sigma^2 1\bar{\delta}^1_+)-0.16(1\sigma^2 2\sigma^2 4\bar{\sigma}^1 1\delta^1_+)](1\pi_x^2 1\pi_y^2 2\pi_y^1 1\delta^1_-)\rangle$$
$$+|1\sigma^2 2\sigma^2 3\sigma^1 1\delta^1_+ 1\pi_x^2[0.30(1\pi_y^2 2\pi_y^1 1\bar{\delta}^1_-)+0.22(1\pi_y^2 2\bar{\pi}_y^1 1\delta^1_-)]\rangle$$
$$-|1\sigma^2 2\sigma^2 3\sigma^1 1\bar{\delta}^1_+[0.16(1\pi_x^1 2\pi_x^1 1\pi_y^2 2\pi_y^1 1\bar{\delta}^1_-)+0.15(2\pi_x^2 1\pi_y^2 2\pi_y^1 1\delta^1_-)]\rangle$$
$$+|1\sigma^2 2\sigma^1 3\sigma^2 1\delta^1_+[0.15(1\bar{\pi}_x^1 2\bar{\pi}_x^1 1\pi_y^2 2\pi_y^1 1\delta^1_-),+0.14(1\pi_x^2 1\pi_y^2 2\pi_y^1 1\bar{\delta}^1_-)]\rangle=|B_1\rangle,\text{MRCI}).$$

The PEC of this state, Fig. 4, experiences two avoided crossings, one at 4.5 bohr with an incoming $20\,^3\Pi(3)$ state, and a second one just after the equilibrium at 3.05 bohr (*vide supra*) with the $5\,^3\Pi(1)$ state. Therefore the equilibrium character of the $8\,^3\Pi(2)$ state is that of the $20\,^3\Pi(3)$, which has already suffered an avoided crossing (*vide supra*), i.e., $Fe(^5F;M=\pm1)+C(^3P;M=0)$. Adiabatically, the $8\,^3\Pi(2)$ state correlates to $Fe(^5D;M=\pm2)+C(^3P;M=\mp1)$. Our MRCI Mulliken equilibrium populations (in B_1 symmetry)

$$4s^{0.93}4p_z^{0.19}3d_{z^2}^{1.35}3d_{xz}^{1.31}4p_x^{0.04}3d_{yz}^{1.73}4p_y^{0.10}3d_{x^2-y^2}^{1.00}3d_{xy}^{1.00}/$$
$$2s^{1.72}2p_z^{0.76}2p_x^{0.64}2p_y^{1.12},$$

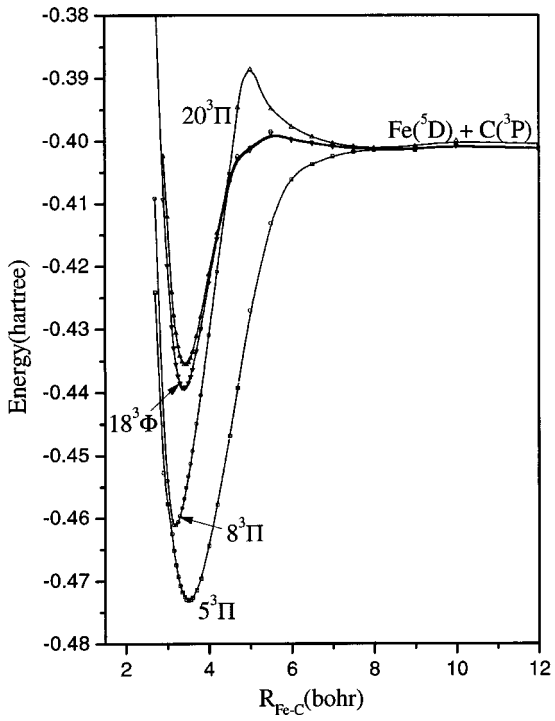

FIG. 4. MRCI potential-energy curves of the triplets $5\,^3\Pi(1)$, $8\,^3\Pi(2)$, $18\,^3\Phi(1)$, and $20\,^3\Pi(3)$, of the FeC molecule.

imply a π bond ($3d_{xz}+2p_x$ in B_1 symmetry), and a σ bond caused by the transfer of 0.5 e^- from the $(4s4p_z3d_z2)^{3.0}$ hybrid on Fe to the $2p_z$ on C. A valence–bond–Lewis (vbL) diagram captures the above description

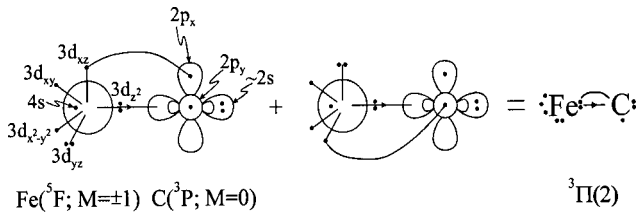

The bonding is similar to that of the $5\,^3\Pi(1)$ state, the difference being that in the present state the σ bond is formed by a $3d_z{}^2\rightarrow2p_z$ transfer, while in the $5\,^3\Pi(1)$ state by a $4s\rightarrow2p_z$ transfer.

The MRCI D_e value with respect to the adiabatic products is 37.8 kcal/mol, while with respect to the diabatic fragments $Fe(^5F)+C(^3P)$ (internal bond strength), we obtain $37.8+\Delta E(^5F\leftarrow{}^5D)=62.0$ kcal/mol.

$$16\,^3\Sigma^-(2)(\sim|[0.43(1\sigma^2 2\sigma^2 3\bar{\sigma}^1 4\sigma^1)$$
$$+0.26(1\sigma^2 2\sigma^1 3\sigma^1 4\bar{\sigma}^1)-0.17(1\sigma^2 2\sigma^2 3\sigma^2)]$$
$$\times(1\pi_x^2 1\pi_y^2 1\delta^1_+ 1\delta^1_-)\rangle-0.35|1\sigma^2 2\sigma^2 3\sigma^1 4\sigma^1$$
$$\times 1\pi_x^2 1\pi_y^2 1\delta^1_+ 1\bar{\delta}^1_-\rangle-0.19|1\sigma^2 2\sigma^2 3\bar{\sigma}^1 4\sigma^1$$
$$\times(1\pi_x^1 2\pi_x^1 1\pi_y^2+1\pi_x^2 1\pi_y^1 2\pi_y^1)1\delta^1_+ 1\bar{\delta}^1_-\rangle$$
$$-0.18|1\sigma^2 2\sigma^2 3\sigma^1 4\sigma^1(1\bar{\pi}_x^1,2\bar{\pi}_x^1 1\pi_y^2$$
$$+1\pi_x^2 1\bar{\pi}_y^1 2\bar{\pi}_y^1)1\delta^1_+ 1\delta^1_-\rangle=|A_2\rangle,\text{CASSCF}).$$

Figure 3 shows the MRCI PEC of the $16\,^3\Sigma^-(2)$ state; notice the missing part of the PEC between 3.6 and 4.2 bohr due to severe problems of convergence in this region at the MRCI level. With respect to the adiabatic fragments $Fe(^5D;M=\pm1)+C(^3P;M=\mp1)$ we predict a $D_e=26.0$ kcal/mol, $r_e=1.799$ Å at the MRCI level of theory.

An avoided crossing that should occur in the uncharted region 3.6–4.2 bohr with another (not calculated) $^3\Sigma^-$ state

changes the PEC's character, so at equilibrium the *in situ* atoms are Fe(^5F;M$=\pm1$)+C(^3P;M$=\mp1$). Our CASSCF Mulliken equilibrium distributions are

$$4s^{0.97}4p_z^{0.36}3d_{z^2}^{1.81}3d_{xz}^{1.20}4p_x^{0.03}3d_{yz}^{1.20}4p_y^{0.03}3d_{x^2-y^2}^{1.00}3d_{xy}^{1.00}/$$
$$2s^{1.77}2p_z^{1.07}2p_x^{0.76}2p_y^{0.76}.$$

Clearly, we have two π bonds and a charge transfer of 0.52 e^- from the metal to the carbon atom along the π frame; as to the σ frame a 0.16 e^- transfer from C to Fe is observed, but we cannot assert the existence of a σ bond. Pictorially

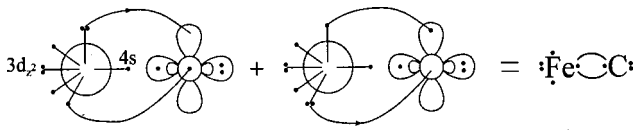

with the $3d_{x^2-y^2}(\delta_+)$, $3d_{xy}(\delta_-)$, $3d_{z^2}(3d_\sigma)$ and $2p_z$ electrons coupled into a triplet.

$$18\,^3\Phi(1)(\sim|1\sigma^2 2\sigma^2 3\sigma^2[0.45(1\pi_x^1 1\pi_y^2 1\delta_+^1 1\delta_-^2$$
$$+1\pi_x^2 1\pi_y^1 1\delta_+^2 1\delta_-^1)$$
$$+0.32(1\pi_x^1 1\pi_y^1 2\bar{\pi}_y^1 1\delta_+^1 1\delta_-^2)$$
$$+0.26(1\pi_x^1 2\bar{\pi}_x^1 1\delta_+^1 \pi_y^1 1\delta_+^2 1\delta_-^1)-0.15$$
$$\times(1\pi_x^1 2\pi_y^2 1\delta_+^1 1\delta_-^2+2\pi_x^2 1\pi_y^1 1\delta_+^2 1\delta_-^1)]\rangle$$
$$=|B_1\rangle,\text{CASSCF}).$$

Adiabatically, this $^3\Phi(1)$ state correlates to Fe (^5D;M $=\pm2$)+C(^3P;±1), Fig. 4. In conjunction with the CASSCF equilibrium population densities

$$4s^{1.22}4p_z^{0.22}3d_{z^2}^{1.39}3d_{xz}^{0.98}4p_x^{0.02}3d_{yz}^{0.98}4p_y^{0.02}(3d_{x^2-y^2}3d_{xy})^{2.98}/$$
$$2s^{1.83}2p_z^{1.32}2p_x^{0.54}2p_y^{0.54},$$

and the leading configurations, we can claim that the bonding is comprised of 3/2 π bonds, and one σ bond (3σ orbital) due to the interaction of the $(4s4p_z3d_z2)^{3.0}$ hybrid on Fe and the $2p_z$ orbital on C. A vbL icon consistent with the previous discussion is the following

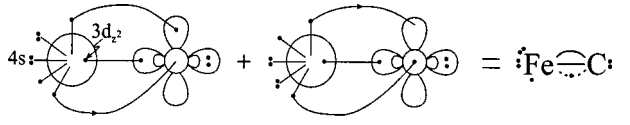

The existing experimental results for a $^3\Phi$ state[11] do not agree with our findings (Table II). As a matter of fact it seems that the experimental assignement is not correct. Considering the overall good to very good agreement with all other experimental results on this system, we believe that a re-evaluation of the experimental findings is in order.

$20\,^3\Pi(3)$. The leading CFs are the same with those of the previously described $18\,^3\Phi(1)$ state, but with the (0.45, 0.45, 0.32, 0.26) vector of coefficients changed to (0.39, −0.39, 0.37, −0.29). As the two atoms come together from infinity, Fe(^5D;M$=0$)+C(^3P;M$=\pm1$), an avoided crossing occurs at 5 bohr with a (not calculated) $^3\Pi(4)$ state, imparting its character of Fe(^5F;M$=\pm1$)+C(^3P;M$=0$) to the $^3\Pi(3)$ curve and resulting to a 7.4 kcal/mol barrier (Fig. 4). A second avoided crossing occurs at about 4.5 bohr with the $8\,^3\Pi(2)$ state (*vide supra*). As a result of the second crossing the *in situ* equilibrium atoms are Fe(^5D;M$=\pm2$) +C(^3P;M$=\mp1$). Populations and bonding are identical with the $18\,^3\Phi(1)$ state; numbers are presented in Table II.

$$29\,^3\Delta(3)(\sim|[0.50(1\sigma^2 2\sigma^1 3\sigma^2)$$
$$-0.24(1\sigma^2 2\sigma^1 3\bar{\sigma}^1 4\sigma^1)]1\pi_x^2 1\pi_y^2 1\delta_+^1 1\delta_-^2\rangle$$
$$+0.22|1\sigma^2 2\sigma^1 3\bar{\sigma}^1(1\pi_x^2 1\pi_y^1 2\pi_y^1$$
$$+1\pi_x^1 2\pi_x^1 1\pi_y^2)1\delta_+^1 1\delta_-^2\rangle-0.20|1\sigma^2 2\sigma^2 3\sigma^1$$
$$\times(1\bar{\pi}_x^1 2\pi_x^1 1\pi_y^2+1\pi_x^2 1\bar{\pi}_y^1 2\pi_y^1)1\delta_+^1 1\delta_-^2\rangle$$
$$=|A_1\rangle,\text{CASSCF})$$

and

$$33\,^3\Delta(4)(\sim|1\sigma^2 2\sigma^1 3\sigma^2[0.46(1\pi_x^2 1\pi_y^2)-0.22$$
$$\times(1\bar{\pi}_x^1 2\pi_x^1 1\pi_y^2+1\pi_x^2 1\bar{\pi}_y^1 2\pi_y^1)1\delta_+^1 1\delta_-^2]\rangle$$
$$-0.28|1\sigma^2 2\sigma^2 3\bar{\sigma}^1(1\pi_x^2 1\pi_y^1 2\pi_y^1$$
$$+1\pi_x^1 2\pi_x^1 1\pi_y^2)1\delta_+^1 1\delta_-^2\rangle$$
$$+0.21|1\sigma^2 2\sigma^1 3\sigma^1 4\sigma^1 1\pi_x^2 1\pi_y^2 1\bar{\delta}_+^1 1\delta_-^2\rangle$$
$$=|A_1\rangle,\ \text{CASSCF}).$$

The PECs of the $^3\Delta(3)$ and $^3\Delta(4)$ states are shown in Fig. 3; they correlate to Fe(^5F;M$=\pm2$)+C(^3P;M$=0$) and Fe(^5F;M$=\pm1$)+C(^3P;M$=\pm1$), respectively. Severe technical difficulties did not allow the construction of the complete PECs. In particular, the parts 4.7–4.1 bohr of the $^3\Delta(3)$ PEC, is missing. At the equilibrium the *in situ* atoms seem to be Fe(^5F;M$=\pm1,\mp3$)+C(^3P;M$=\pm1$) for the $^3\Delta(3)$ and $^3\Delta(4)$ states, respectively. In both states, we think, the atoms are held together by two π and one σ bond.

$$34\,^3\Gamma(1)(\sim|1\sigma^2 2\sigma^2 3\sigma^1[0.41(1\pi_x^2 2\bar{\pi}_x^1 1\pi_y^1)$$
$$-0.39(1\bar{\pi}_x^1 1\pi_y^2 2\pi_y^1)]1\delta_+^2 1\delta_-^1\rangle$$
$$-0.19|1\sigma^2 2\sigma^2 3\bar{\sigma}^1(1\pi_x^2 1\pi_y^1 2\pi_y^1$$
$$+1\pi_x^1 2\pi_x^1 1\pi_y^2)1\delta_+^1 1\delta_-^2\rangle=|A_1\rangle,\ \text{CASSCF}).$$

This state correlates to Fe(^5F;M$=\pm3$)+C(^3P;M$=\pm1$). As Fig. 3 shows, we were unable to construct its complete PEC due to technical difficulties. As a matter of fact the PEC's part from 5.0 to 3.6 bohr is missing. Even around equilibrium our PEC is not ''smooth'' enough. It seems that

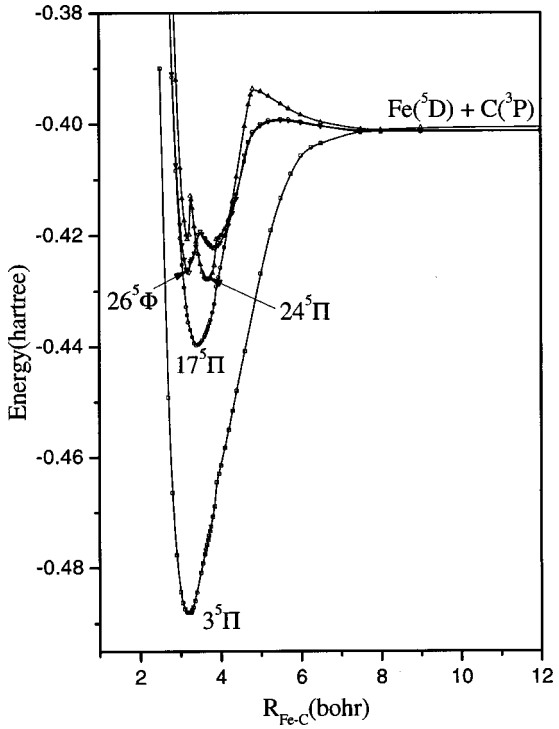

FIG. 5. MRCI potential-energy curves of the quintets $3\,^5\Pi(1)$, $17\,^5\Pi(2)$, $24\,^5\Pi(3)$, and $26\,^5\Phi(1)$.

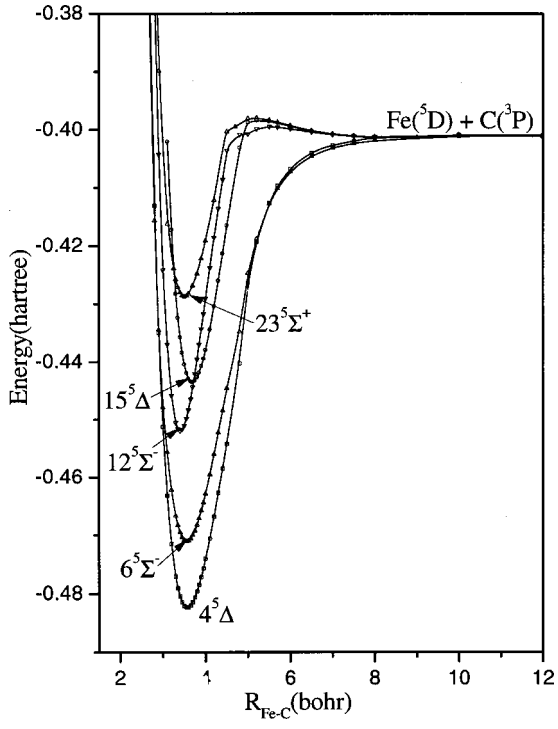

FIG. 6. MRCI potential-energy curves of the quintets $4\,^5\Delta(1)$, $6\,^5\Sigma^-(1)$, $12\,^5\Sigma^-(2)$, $15\,^5\Delta(2)$, and $23\,^5\Sigma^+(1)$.

the *in situ* equilibrium atoms carry the same character with the asymptotic fragments and the bonding appears to consist of a 1/2 π and one σ bond.

Finally, we would like to mention our unsuccessful efforts to compute a $^3\Sigma^+(1)$ state. Its asymptotic fragments are $\mathrm{Fe}(^5D;\mathrm{M}=\pm1)+\mathrm{C}(^3P;\mathrm{M}=\mp1)$, and we were only able to construct its PEC from infinity to 4.3 bohr and from 3.4 to 2.5 bohr (Fig. 3). However, we do not have any points close to equilibrium position, which we surmise to be at about 3.6 bohr.

B. Quintets: $3\,^5\Pi(1)$, $4\,^5\Delta(1)$, $6\,^5\Sigma^-(1)$, $12\,^5\Sigma^-(2)$, $15\,^5\Delta(2)$, $17\,^5\Pi(2)$, $23\,^5\Sigma^+(1)$, $24\,^5\Pi(3)$, and $26\,^5\Phi(1)$

$$3\,^5\Pi(1)(\sim|1\sigma^2 2\sigma^2 3\sigma^1[0.77(1\pi_x^2) - 0.17(2\pi_x^2)]1\pi_y^2 2\pi_y^1 1\delta_+^1 1\delta_-^1\rangle=|B_1\rangle,\ \text{MRCI}).$$

The asymptotic fragments are $\mathrm{Fe}(^5D;\mathrm{M}=\pm1)+\mathrm{C}(^3P;\mathrm{M}=0)$. It seems that around 4 bohr an interaction takes place with the $17\,^5\Pi(2)$ state, which already had experienced an avoided crossing with the $24\,^5\Pi(3)$ state. The result is a rather rough shaped $3\,^5\Pi(1)$ PEC around this region and the character transmission of the $24\,^5\Pi(3)$ to the equilibrium region of the $3\,^5\Pi(1)$, i.e., $\mathrm{Fe}(^5F;\mathrm{M}=\pm1)+\mathrm{C}(^3P;\mathrm{M}=0)$; see Fig. 5. The Mulliken MRCI densities (B_1 symmetry)

$$4s^{0.87}4p_z^{0.26}3d_{z^2}^{1.26}3d_{xz}^{1.37}4p_x^{0.04}3d_{yz}^{1.70}4p_y^{0.14}3d_{x^2-y^2}^{1.00}3d_{xy}^{1.00}/ 2s^{1.76}2p_z^{0.80}2p_x^{0.58}2p_y^{1.13},$$

and the leading configuration(s) suggest the formation of a π bond (π_x in B_1 symmetry), a transfer of 0.13 and a promotion of 0.14 e^- from the $3d_{yz}$ to $2p_y$ and $4p_y$, respectively, and the formation of a σ bond by transfer of 0.56 e^- from the $(3d_{z^2})^{2.0}$ of Fe to the empty $2p_z$ orbital of C. We can draw the following bonding diagram

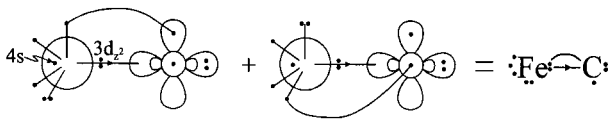

$\mathrm{Fe}(^5\mathrm{F};\ \mathrm{M}=\pm1)$ $\mathrm{C}(^3\mathrm{P};\ \mathrm{M}=0)$ $^5\Pi(1)$

With the exception of ω_e our results are in agreement with the results of Hirano and co-workers,[7] but in disagreement with the findings of SG[6] (Table II). Certainly the DFT D_e result of 138 kcal/mol[8] is flatly wrong, as is clear from our $D_e=54.6$ (59.2) kcal/mol at the MRCI(+Q) level of theory. Finally, the recent experimental assignment to a $^5\Pi$ state,[14] 3460 cm^{-1} (9.89 kcal/mol) above the X state, is questionable; instead this transition points to the $1\,^1\Delta$ state, the first excited state of the FeC species; see Table II (*vide infra*).

$$4\,^5\Delta(1)(\sim|1\sigma^2 2\sigma^2 3\sigma^1[0.38(1\pi_x^2 1\pi_y^1 2\pi_y^1+1\pi_x^1 2\pi_x^1 1\pi_y^2) - 0.23(2\pi_x^2 1\pi_y^1 2\pi_y^1+1\pi_x^1 2\pi_x^1 2\pi_y^2) + 0.21(1\bar{\pi}_x^1 2\pi_x^1 1\pi_y^1 2\pi_y^1)]1\delta_+^1 1\delta_-^2\rangle + 0.28|1\sigma^2 2\sigma^1 3\sigma^1 4\sigma^1 1\pi_x^2 2\pi_y^2 1\delta_+^1 1\delta_-^2\rangle + 0.17|1\sigma^2 2\bar{\sigma}^1 3\sigma^1 4\sigma^1(1\pi_x^1 2\pi_x^1 1\pi_y^2 + 1\pi_x^2 1\pi_y^1 2\pi_y^1)1\delta_+^1 1\delta_-^2\rangle=|A_1\rangle,\ \text{CASSCF}.$$

In A_2 the $1\delta_+^1 1\delta_-^2$ distribution becomes $1\delta_+^2 1\delta_-^1$).

Asymptotically we have $|4\,^5\Delta(1)\rangle=|^5D;\mathrm{M}=\pm2\rangle_{\mathrm{Fe}} \times|^5D;\mathrm{M}=0\rangle_{\mathrm{C}}$, with the corresponding PEC shown in Fig. 6

and numerical results presented in Table II along with the results of SG.[6] The CASSCF Mulliken population analysis (A_1 symmetry)

$$4s^{0.95}4p_z^{0.34}3d_{z^2}^{1.07}3d_{xz}^{1.05}4p_x^{0.04}3d_{yz}^{1.05}4p_y^{0.04}3d_{x^2-y^2}^{1.00}3d_{xy}^{2.00}/$$
$$2s^{1.78}2p_z^{0.86}2p_x^{0.90}2p_y^{0.90}$$

in conjunction with the CFs shown in the above-mentioned, suggests the following vbL icon (A_1 symmetry)

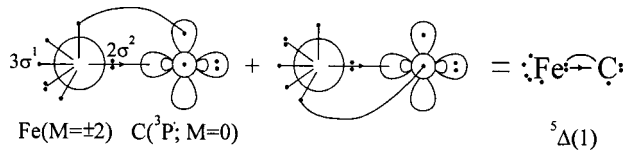

or a π bond with $\sim$0.2 e^- migrating from C to Fe via the π frame, and a σ dative bond originating from the Fe $(4s4p_z3d_{z^2})^{3.0}$ hybrid; 0.64 e^- are transferred from this hybrid to the empty $2p_z$ C orbital.

$$6^5\Sigma^-(1)(\sim|1\sigma^2 2\sigma^2 3\sigma^2[0.40(1\pi_x^2 1\pi_y^1 2\pi_y^1 + 1\pi_x^1 2\pi_x^1 1\pi_y^2)$$
$$-0.24(2\pi_x^2 1\pi_y^1 2\pi_y^1 + 1\pi_x^1 2\pi_x^1 2\pi_y^2)$$
$$+0.18(1\overline{\pi}_x^1 2\pi_x^1 1\pi_y^1 2\pi_y^1)1\delta_+^1 1\delta_-^1\rangle$$
$$-0.25|1\sigma^2 2\sigma^1 3\sigma^1 4\sigma^1 1\pi_x^2 2\pi_y^2 1\delta_+^1 1\delta_-^1\rangle$$
$$-0.20|1\sigma^2 2\sigma^2 3\sigma^2 1\pi_x^1 2\pi_x^1 1\pi_y^1 2\pi_y^1 1\delta_+^1 1\delta_-^1\rangle$$
$$=|A_2\rangle,\ \text{CASSCF}).$$

This state traces its ancestry to Fe(^5D;M=0) + C(^3P;M=0) as shown in Fig. 6. In Table II our results are contrasted with the results of SG,[6] where we observe significant differences, particularly between the μ (1.71 versus 2.12 D), and T_e (35.8 versus 23.5 kcal/mol) values.

The equilibrium CASSCF atomic Mulliken distributions are

$$4s^{1.08}4p_z^{0.32}3d_{z^2}^{1.95}3d_{xz}^{1.06}4p_x^{0.04}3d_{yz}^{1.06}4p_y^{0.04}3d_{x^2-y^2}^{1.00}3d_{xy}^{1.00}/$$
$$2s^{1.79}2p_z^{0.85}2p_x^{0.89}2p_y^{0.89}.$$

We can claim that the atoms are held together by a π and a σ bond; the latter is due to a transfer of 0.64 e^- from a $(4s4p_z)^{2.0}$ hybrid on Fe to the empty $2p_z$ orbital of carbon. In pictures

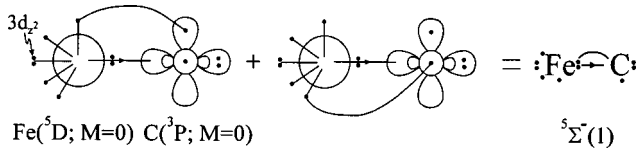

$$12^5\Sigma^-(2)(\sim|1\sigma^2 2\sigma^2 3\sigma^1 4\sigma^1[0.51(1\pi_x^2 1\pi_y^2 1\delta_+^1 1\delta_-^1)$$
$$-0.18(1\pi_x^2 1\pi_y^1 2\pi_y^1 + 1\pi_x^1 2\pi_x^1 1\pi_y^2)1\delta_+^1 1\overline{\delta}_-^1]\rangle$$
$$-|[0.26(1\sigma^2 2\sigma^2 3\sigma^2) + 0.18(1\sigma^2 2\sigma^2 3\overline{\sigma}^1 4\sigma^1)]$$
$$\times(1\pi_x^2 1\pi_y^1 2\pi_y^1 + 1\pi_x^1 2\pi_x^1 1\pi_y^2)1\delta_+^1 1\delta_-^1\rangle$$
$$=|A_2\rangle,\ \text{CASSCF}).$$

The adiabatic fragments are Fe(^5D;M=$\pm$1)+C(^3P;M=$\mp$1); as we move toward the equilibrium and around 4.8 bohr, an avoided crossing occurs with a (not calculated) $^5\Sigma^-(3)$ state correlating to Fe(^5F;M=$\pm$1)+C(^3P;M=$\mp$1), Fig. 6, transferring its character at the same time to the equilibrium atoms. The CASSCF populations,

$$4s^{1.01}4p_z^{0.38}3d_{z^2}^{1.65}3d_{xz}^{1.23}4p_x^{0.03}3d_{yz}^{1.23}4p_y^{0.03}3d_{x^2-y^2}^{1.00}3d_{xy}^{1.00}/$$
$$2s^{1.80}2p_z^{1.13}2p_x^{0.74}2p_y^{0.74},$$

in conjunction with the leading CFs reveal two π bonds and a *repulsive* σ interaction. The bonding is succinctly represented in the vbL icon that follows

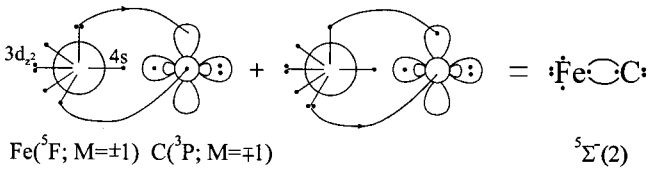

$$15^5\Delta(2)(\sim|[0.28(1\sigma^2 2\sigma^2 3\sigma^1) - 0.20(1\sigma^2 2\overline{\sigma}^1 3\sigma^1 4\sigma^1)$$
$$+0.18(1\sigma^2 2\sigma^2 4\sigma^1)](1\pi_x^2 1\pi_y^1 2\pi_y^1$$
$$+1\pi_x^1 2\pi_x^1 1\pi_y^2)1\delta_+^1 1\delta_-^2\rangle + |[0.27(1\sigma^2 2\overline{\sigma}^1 3\sigma^2)$$
$$-0.17(1\sigma^2 2\overline{\sigma}^1 3\sigma^1 4\overline{\sigma}^1)]1\pi_x^1 2\pi_x^1 1\pi_y^1 2\pi_y^1 1\delta_+^1 1\delta_-^2\rangle$$
$$-0.19|1\sigma^2 2\sigma^1 3\sigma^1 4\sigma^1 1\pi_x^2 1\pi_y^2 1\delta_+^1 1\delta_-^2\rangle$$
$$-0.17|1\sigma^2 2\sigma^1 3\sigma^2(2\pi_x^2 1\pi_y^1 2\pi_y^1 + 1\pi_x^1 2\pi_x^1 2\pi_y^2)$$
$$\times 1\delta_+^1 1\delta_-^2\rangle = |A_1\rangle,\ \text{CASSCF}).$$

As we approach from infinity [Fe(^5D;M=$\pm$1) + C(^3P;M=$\pm$1)] toward equilibrium, Fig. 6, the $^5\Delta(2)$ suffers an avoided crossing at 4.5 bohr with the (not calculated) $^5\Delta(3)$ state, the latter correlating to Fe(^5F;M=$\pm$2) + C(^3P;M=0). An "interaction" also occurs with the lower $4\,^5\Delta(1)$ state at about 4 bohr. The CASSCF populations and bonding are similar to that of the $4\,^5\Delta(1)$ state (*vide supra*), i.e., a π and a σ bond keep the two atoms together.

$$17^5\Pi(2)(\sim|[0.54(1\sigma^2 2\sigma^1 3\sigma^2) - 0.27(1\sigma^2 2\sigma^1 3\overline{\sigma}^1 4\sigma^1)$$
$$-0.17(1\sigma^2 2\sigma^2 4\sigma^1)]1\pi_x^2 1\pi_y^2 2\pi_y^1 1\delta_+^1 1\delta_-^1\rangle$$
$$+[0.25(1\sigma^2 2\sigma^2 3\overline{\sigma}^1 1\pi_x^1 2\pi_x^1)$$
$$-0.17(1\sigma^2 2\sigma^1 3\sigma^2 2\pi_x^2)]1\pi_y^2 2\pi_y^1 1\delta_+^1 1\delta_-^1\rangle$$
$$-|1\sigma^2 2\sigma^1 3\sigma^2 1\pi_x^1 2\pi_x^1 1\pi_y^2 2\pi_y^1[0.22(1\overline{\delta}_+^1 1\delta_-^1)$$
$$+0.19(1\delta_+^1 1\overline{\delta}_-^1)]\rangle = |B_1\rangle,\ \text{MRCI}).$$

The adiabatic fragments are Fe(^5D;M=$\pm$2)+C(^3P;M=$\mp$1). Moving to the left from infinity an avoided crossing takes place with the $24\,^5\Pi(3)$ state at 4.4 bohr; a second avoided crossing occurs around 4 bohr with the $3\,^5\Pi(1)$ state; see Fig. 5. Due to the two consecutive avoided crossing the *in situ* equilibrium atoms are Fe(^5D;M=$\pm$1) + C(^3P;M=0). The MRCI Mulliken populations (symmetry B_1) are

$$4s^{1.08}4p_z^{0.24}3d_{z^2}^{1.14}3d_{xz}^{1.18}4p_x^{0.06}3d_{yz}^{1.86}4p_y^{0.09}3d_{x^2-y^2}^{1.00}3d_{xy}^{1.00}/$$
$$2s^{1.68}2p_z^{0.80}2p_x^{0.76}2p_y^{1.03}.$$

The bonding is similar to that of the $3\,^5\Pi(1)$ state, the difference being that in the present state the σ bond is due a $4s^2(\mathrm{Fe})\rightarrow 2p_z(\mathrm{C})$ instead of $3d_{z^2}(\mathrm{Fe})\rightarrow 2p_z(\mathrm{C})$ electron transfer.

$$23\,^5\Sigma^+(1)(\sim|1\sigma^2 2\sigma^2 3\sigma^1\{[0.34(1\pi_x^1 2\pi_x^1 1\pi_y^2 - 1\pi_x^2 1\pi_y^1 \times 2\pi_y^1) + 0.18(1\pi_x^1 2\pi_x^1 1\bar{\pi}_y^1 2\pi_y^1)]1\delta_+^1 1\delta_-^2 + 0.34(1\pi_x^1 1\pi_y^2 2\pi_y^1 - 1\pi_x^2 2\pi_x^1 1\pi_y^1)1\delta_+^1 1\delta_-^1\}\rangle = |A_1\rangle,\ \mathrm{MRCI}).$$

At infinity we have $\mathrm{Fe}(^5D;\mathrm{M}=\pm 1)+\mathrm{C}(^3P;\mathrm{M}=\mp 1)$. As we approach the PEC's minimum and around 4.5 bohr, an avoided crossing takes place with the higher (not calculated) $^5\Sigma^+(2)$ state resulting to a barrier of 2 kcal/mol with respect to the asymptotic products (Fig. 6), and a character change of the *in situ* equilibrium atoms to $\mathrm{Fe}(^5F;\mathrm{M}=\pm 1)+\mathrm{C}(^3P;\mathrm{M}=\mp 1)$. Our MRCI atomic Mulliken populations and leading CFs

$$4s^{0.93}4p_z^{0.26}3d_{z^2}^{1.15}3d_{xz}^{1.11}4p_x^{0.07}3d_{yz}^{1.11}4p_y^{0.07}3d_{x^2-y^2}^{1.46}3d_{xy}^{1.46}/ 2s^{1.79}2p_z^{0.89}2p_x^{0.81}2p_y^{0.82}$$

imply a σ and a π bond as shown in the bonding diagram

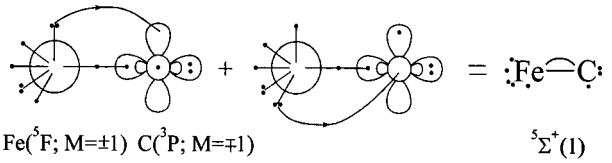

The cause of the σ bond is a 0.3 e^- transfer from the p_z orbital on C to the $(4s4p_z3d_{z^2})^{2.0}$ hybrid on Fe; to the opposite direction and via the π frame 0.63 e^- migrate from the Fe to C giving rise to the π bond.

$$24\,^5\Pi(3)(\sim|1\sigma^2 2\sigma^2 3\sigma^1[0.45(1\pi_x^1 2\pi_x^1 1\pi_y^2 2\bar{\pi}_y^1) + 0.33(1\pi_x^2 1\pi_y^1 2\pi_y^2) - 0.32(1\pi_x^2 1\pi_y^2 2\pi_y^1)]1\delta_+^1 1\delta_-^1\rangle - |1\sigma^2 2\sigma^1 3\sigma^1 4\sigma^1[0.27(1\pi_x^2 1\pi_y^2 2\bar{\pi}_y^1 1\delta_+^1 1\delta_-^1) - 0.24(1\pi_x^1 2\pi_x^1 1\pi_y^2 2\bar{\pi}_y^1 1\bar{\delta}_+^1 1\delta_-^1)]\rangle = |B_1\rangle,$$

MRCI, global (G) minimum).

This is a complicated state whose PEC, shown in Fig. 5, suffers multiple avoided crossings. Moving from infinity, $\mathrm{Fe}(^5D;\mathrm{M}=0)+\mathrm{C}(^3P;\mathrm{M}=\pm 1)$, toward equilibrium, the first avoided crossing occurs at 4.8 bohr with an incoming (not calculated) $^5\Pi$ state correlating to $\mathrm{Fe}(^5F;\mathrm{M}=\pm 1)+\mathrm{C}(^3P;\mathrm{M}=0)$, and giving rise to a barrier of 4.2 kcal/mol with respect to the asymptote. Moving further to the left, a second avoided crossing takes place at 4.4 bohr with the $17\,^5\Pi(2)$ state (*vide supra*) correlating to $\mathrm{Fe}(^5D;\mathrm{M}=\pm 2)+\mathrm{C}(^3P;\mathrm{M}=\mp 1)$. At 3.9 bohr a third avoided crossing intervenes with a $^5\Pi$ state of unknown lineage; in addition, it interacts with the previously mentioned $17\,^5\Pi(2)$ state at about 3.7 bohr. Therefore, at the (G) minimum the identities of the *in situ* atoms are not clear. Perhaps we can say that the bonding is of $\sigma^2\pi^2$ character. Passing equilibrium, $r_e=3.677$ bohr, the $24\,^5\Pi(3)$ state suffers a fourth avoided crossing at 3.25 bohr with another $^5\Pi$ state of, also unknown origin, resulting to a formal (L) minimum at $r_e=3.19$ bohr, Fig. 5.

$$26\,^5\Phi(1)(\sim 0.56|1\sigma^2 2\sigma^1 3\sigma^1 1\pi_x^2(2\pi_x^1 1\pi_y^2 1\delta_+^1 1\delta_-^2 + 1\pi_y^2 2\pi_y^1 1\delta_+^2 1\delta_-^1)\rangle = |B_1\rangle,\ \mathrm{CASSCF},\ \mathrm{global}\ (\mathrm{G})\ \mathrm{minimum}).$$

This state correlates to $\mathrm{Fe}(^5D;\mathrm{M}=\pm 2)+\mathrm{C}(^3P;\mathrm{M}=\pm 1)$, maintaining this character up to the first local (L) minimum, $r_e=3.838$ bohr, Fig. 5, and $D_e=13.1$ kcal/mol; see Table II. Due to an avoided crossing at 3.5 bohr with the (not calculated) $^5\Phi(2)$ state correlating to $\mathrm{Fe}(^5F;\mathrm{M}=\pm 3)+\mathrm{C}(^3P;\mathrm{M}=0)$, these atomic characters are transferred to the global (G) minimum at $r_e=3.203$ bohr. The MRCI atomic populations of the L and G minima are given below:

$$\mathrm{L:}\ 4s^{1.03}4p_z^{0.43}3d_{z^2}^{1.08}3d_{xz}^{1.04}4p_x^{0.03}3d_{yz}^{1.04}4p_y^{0.03}3d_{x^2-y^2}^{1.49}3d_{xy}^{1.49}/ 2s^{1.81}2p_z^{1.47}2p_x^{0.50}2p_y^{0.50}$$

$$\mathrm{G:}\ 4s^{0.79}4p_z^{0.16}3d_{z^2}^{0.86}3d_{xz}^{1.35}4p_x^{0.09}3d_{yz}^{1.35}4p_y^{0.09}3d_{x^2-y^2}^{1.48}3d_{xy}^{1.48}/ 2s^{1.69}2p_z^{0.56}2p_x^{1.00}2p_y^{1.00}.$$

Notice the totally different distributions of the C atom between the L and G "isomers" characteristic of the $\mathrm{M}=\pm 1$, and $\mathrm{M}=0$ carbon terms, respectively; corresponding differences in the metal are not so distinct. With the help of the populations and leading CFs, the following bonding diagrams can be drawn for the L and G minima, respectively

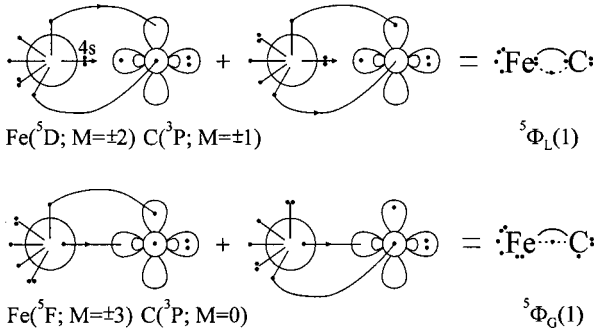

The previous diagrams imply 3/2 π bonds and a strong σ interaction in the L case, and a π and 1/2 σ bond in the G case.

C. Septets: $9\,^7\Delta(1)$, $10\,^7\Pi(1)$, $13\,^7\Sigma^-(1)$, $22\,^7\Delta(2)$, $25\,^7\Pi(2)$, $27\,^7\Sigma^+(1)$, $28\,^7\Sigma^-(2)$, $30\,^7\Pi(3)$, and $31\,^7\Phi(1)$

$9\,^7\Delta(1)$, $22^7\Delta(2)$. Asymptotically, these two states are described by the product wave functions $|^5D;\mathrm{M}=\pm 2\rangle\times|^3P;\mathrm{M}=0\rangle$ and $|^5D;\mathrm{M}=\pm 1\rangle\times|^3P;\mathrm{M}=\pm 1\rangle$, respectively, with their PECs given in Fig. 7. The equilibrium CASSCF leading CFs (symmetry A_1) for the $9\,^7\Delta(1)$ state are

$$9\,^7\Delta(1)(\sim|[0.56(1\sigma^2 2\sigma^1 3\sigma^2)-0.29(1\sigma^2 2\sigma^1 4\sigma^2)-0.21(1\sigma^2 2\sigma^1 3\bar{\sigma}^1 4\sigma^1)-0.12(1\sigma^2 2\sigma^1 3\sigma^1 4\bar{\sigma}^1)$$
$$-0.11(1\sigma^2 2\sigma^2 3\sigma^1)]1\pi_x^1 2\pi_x^1 1\pi_y^1 2\pi_y^1 1\delta_+^1 1\delta_-^2\rangle+|1\sigma^2 2\sigma^1 3\sigma^1 4\sigma^1\{[-0.39(1\pi_x^2 1\pi_y^1 2\pi_y^1+1\pi_x^1 2\pi_x^1 1\pi_y^2)$$
$$+0.27(2\pi_x^2 1\pi_y^1 2\pi_y^1+1\pi_x^1 2\pi_x^1 2\pi_y^2)-0.09(1\bar{\pi}_x^1 2\pi_x^1 1\pi_y^1 2\pi_y^1)]\delta_+^1 1\delta_-^2+0.24(1\pi_x^1 2\pi_x^1 1\pi_y^1 2\pi_y^1 1\bar{\delta}_+^1 1\delta_-^2)\}\rangle).$$

For the $22\,^7\Delta(2)$ state the CFs are the same, but the corresponding vector coefficients are 0.58, −0.27, 0.39, 0.23, 0.19, 0.24, −0.17, −0.20, and −0.26. The *repulsive character* of the $22\,^7\Delta(2)$ state, Fig. 7, is interrupted at 4.7 bohr where an avoided crossing occurs with an incoming $^7\Delta$ state, possibly correlating to $Fe^+(^6D;M=\pm 2)+C^-(^4S)$, (experimentally) 6.2 eV higher than the ground-state neutral atoms. The ionic character is imparted to the equilibrium of this state ($r_e=2.081$ Å, Table II), and perhaps to the $9\,^7\Delta(1)$ state through an interaction between the two $^7\Delta$ states around 4.5 bohr. The atomic CASSCF populations of the two states are practically identical, those of the $9\,^7\Delta(1)$ being

$$4s^{0.97}4p_z^{0.38}3d_{z^2}^{1.04}3d_{xz}^{1.02}4p_x^{0.04}3d_{yz}^{1.02}4p_y^{0.04}3d_{x^2-y^2}^{1.00}3d_{xy}^{2.00}/$$
$$2s^{1.76}2p_z^{0.85}2p_x^{0.93}2p_y^{0.93}.$$

The bonding for both states can be described pictorially by the following superposition of vbL icons, indicating in essence the formation of a single σ bond and the transfer of about 0.5 e^- from Fe to C

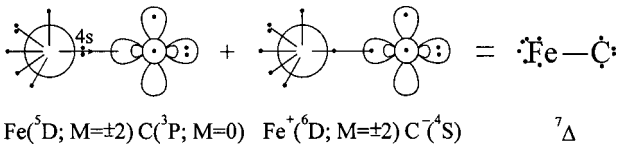

While the r_e, ω_e, and μ values of SG[6] are in relative good agreement with ours (Table II), there is complete disagreement between the T_e values, the present one being twice as large.

$$10\,^7\Pi(1)(\sim|[0.53(1\sigma^2 2\sigma^2 3\sigma^1)+0.26(1\sigma^2 2\sigma^1 3\bar{\sigma}^1 4\sigma^1)]$$
$$\times 1\pi_x^1 2\pi_x^1 1\pi_y^2 2\pi_y^1 1\delta_+^1 1\delta_-^1\rangle$$
$$-|1\sigma^2 2\sigma^1 3\sigma^1 4\sigma^1 1\pi_x^1\{[0.45(2\bar{\pi}_x^1 1\pi_y^2 2\pi_y^1)$$
$$+0.34(2\pi_x^1 1\pi_y^2 2\bar{\pi}_y^1)]1\delta_+^1 1\delta_-^1$$
$$-2\pi_x^1 1\pi_y^2 2\pi_y^1[0.39(1\bar{\delta}_+^1 1\delta_-^1)+0.21(1\delta_+^1 1\bar{\delta}_-^1)]\}\rangle$$
$$=|B_1\rangle,\text{CASSCF}).$$

Asymptotically, we have $Fe(^5D;M=\pm 1)+C(^3P;M=0)$ and this character is conserved up to the equilibrium; the PEC is shown in Fig. 8. An avoided crossing exists in the repulsive part of the PEC around 3.1 bohr with the $25\,^7\Pi(2)$ (*vide infra*). The CASSCF atomic distributions are the following

$$4s^{1.00}4p_z^{0.34}3d_{z^2}^{1.05}3d_{xz}^{1.03}4p_x^{0.04}3d_{yz}^{2.00}4p_y^{0.04}3d_{x^2-y^2}^{1.00}3d_{xy}^{1.00}/$$
$$2s^{1.78}2p_z^{0.82}2p_x^{0.92}2p_y^{0.94}.$$

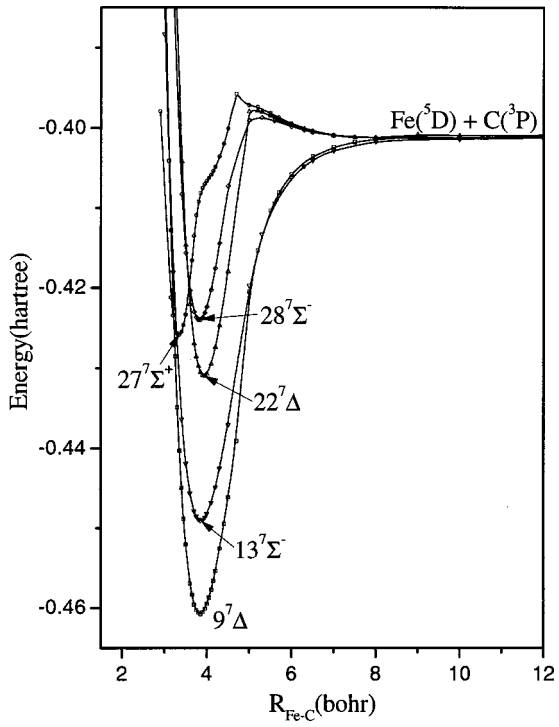

FIG. 7. MRCI potential-energy curves of the septets $9\,^7\Delta(1)$, $13\,^7\Sigma^-(1)$, $22\,^7\Delta(2)$, $27\,^7\Sigma^+(1)$, and $28\,^7\Sigma^-(2)$.

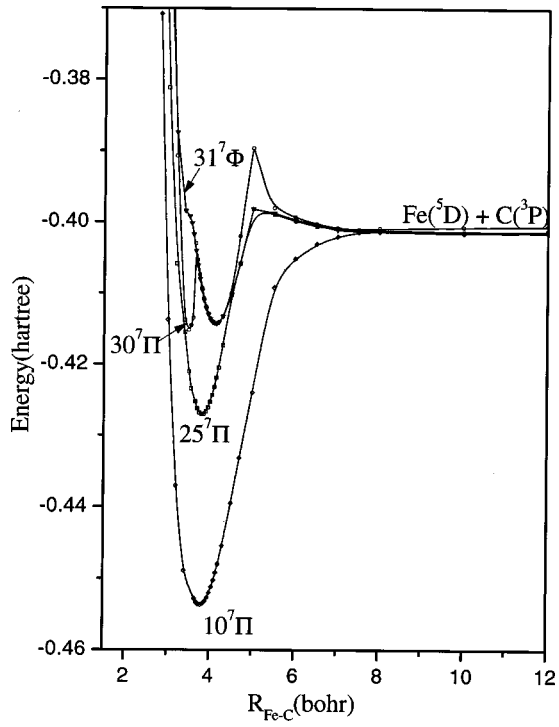

FIG. 8. MRCI potential-energy curves of the septets $10\,^7\Pi(1)$, $25\,^7\Pi(2)$, $30\,^7\Pi(3)$, and $31\,^7\Phi(1)$.

The examination of the leading CFs in conjunction with the Mulliken analysis indicates the formation of a σ bond according to the scheme (B_1 symmetry)

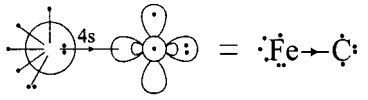

$\mathrm{Fe}(^5\mathrm{D};\mathrm{M}=\pm1)\ \ \mathrm{C}(^3\mathrm{P};\mathrm{M}=0)\qquad {}^7\Pi(1)$

Again, a strong disagreement is observed between our T_e value and the value of SG[6] (Table II).

$$13\,{}^7\Sigma^-(1)(\sim|[0.63(1\sigma^2 2\sigma^2 3\sigma^2)-0.30(1\sigma^2 2\sigma^2 4\sigma^2)]\times 1\pi_x^1 2\pi_x^1 1\pi_y^1 2\pi_y^1 1\delta_+^1 1\delta_-^1\rangle$$
$$-|1\sigma^2 2\sigma^2 3\sigma^1 4\sigma^1[0.37(1\pi_x^1 2\pi_x^1 1\pi_y^2+1\pi_x^2 1\pi_y^1 2\pi_y^1)$$
$$-0.25(1\pi_x^1 2\pi_x^1 2\pi_y^2+2\pi_x^2 1\pi_y^1 2\pi_y^1]1\delta_+^1 1\delta_-^1$$
$$-0.21(1\pi_x^1 2\pi_x^1 1\pi_y^1 2\pi_y^1 \delta_+^1 1\bar{\delta}_-^1)\}\rangle=|A_2\rangle,\mathrm{CASSCF}).$$

The asymptotic description is $\mathrm{Fe}(^5D;\mathrm{M}=0)+\mathrm{C}(^3P;\mathrm{M}=0)$, and the same character prevails in the equilibrium, Fig. 7. The atomic Mulliken equilibrium distributions,

$$4s^{1.05}4p_z^{0.35}3d_{z^2}^{1.98}3d_{xz}^{1.03}4p_x^{0.04}3d_{yz}^{1.03}4p_y^{0.04}3d_{x^2-y^2}^{1.00}3d_{xy}^{1.00}/$$
$$2s^{1.78}2p_z^{0.83}2p_x^{0.93}2p_y^{0.93},$$

clearly indicate the formation of a σ bond with a concomitant transfer of 0.6 e^- from a $(4s4p_z)^{2.0}$ hybrid on Fe to the empty $2p_z$ orbital of C, while $\sim$0.1 e^- are moving back from C to Fe through the π frame. Pictorially,

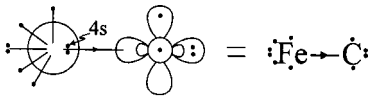

$\mathrm{Fe}(^5\mathrm{D};\mathrm{M}=0)\ \ \mathrm{C}(^3\mathrm{P};\mathrm{M}=0)\qquad {}^7\Sigma(1)$

Finally, as in the previously described $9\,{}^7\Delta(1)$ and $10\,{}^7\Pi(1)$ states, our T_e value is at variance with the corresponding T_e value of the SG work[6] (Table II).

$$25{}^7\Pi(2)(\sim|[0.49(1\sigma^2 2\sigma^1 3\sigma^2)+0.42(1\sigma^2 2\sigma^1 3\sigma^1 4\bar{\sigma}^1)$$
$$+0.35(1\sigma^2 2\sigma^2 3\sigma^1)-0.30(1\sigma^2 2\sigma^1 4\sigma^2)$$
$$-0.21(1\sigma^2 2\sigma^2 4\sigma^1)]1\pi_x^1 2\pi_x^1 1\pi_y^2 2\pi_y^1 1\delta_+^1 1\delta_-^1\rangle$$
$$-|1\sigma^2 2\sigma^1 3\sigma^1 4\sigma^1\{[0.28(1\bar{\pi}_x^1 2\pi_x^1)-0.20(1\pi_x^1 2\bar{\pi}_x^1)]$$
$$\times 1\pi_y^2 2\pi_y^1 1\delta_+^1 1\delta_-^1+1\pi_x^1 2\pi_x^1 1\pi_y^2 2\pi_y^1[0.28(1\delta_+^1 1\bar{\delta}_-^1)$$
$$+0.24(1\bar{\delta}_+^1 1\delta_-^1)]\}\rangle=|B_1\rangle,\mathrm{CASSCF}).$$

As we move from infinity, $\mathrm{Fe}(^5D;\mathrm{M}=\pm2)+\mathrm{C}(^3P;\mathrm{M}=\mp1)$, the $25\,{}^7\Pi(2)$ suffers its first avoided crossing at about 4.5 bohr with the $30\,{}^7\Pi(3)$ state, therefore acquiring at equilibrium the latter's character, $\mathrm{Fe}(^5F;\mathrm{M}=\pm1)+\mathrm{C}(^3P;\mathrm{M}=0)$; see Fig. 8. In the PEC's repulsive part a second avoided crossing occurs around 3.4 bohr again with the $30\,{}^7\Pi(3)$ state, imparting its character to the $25\,{}^7\Pi(2)$ state, $\mathrm{Fe}(^5F;\mathrm{M}=0)+\mathrm{C}(^3P;\mathrm{M}=\pm1)$, and finally, a third avoided crossing takes place at 3.0 bohr with both $10\,{}^7\Pi(1)$ and $30\,{}^7\Pi(3)$ states. Our equilibrium CASSCF atomic populations are practically the same with those of $10\,{}^7\Pi(1)$ (see above-mentioned), indicating the formation of a σ bond caused by the transfer of 0.6 e^- from the hybrid $(3d_z 24p_z)^{2.0}$ on Fe to the empty $2p_z$ orbital of carbon. Also, $\sim$0.1 e^- are fed back to the Fe atom via the π nonbonding frame.

$$27{}^7\Sigma^+(1)(\sim 0.84|1\sigma^2 2\sigma^1 3\sigma^1 1\pi_x^2 2\pi_x^1 1\pi_y^2 2\pi_y^1 1\delta_+^1 1\delta_-^1\rangle$$
$$=|A_1\rangle,\mathrm{MRCI}).$$

The asymptotic products are $\mathrm{Fe}(^5D;\mathrm{M}=\pm1)+\mathrm{C}(^3P;\mathrm{M}=\mp1)$. As we move to the left, the PEC presents a Pauli repulsive interaction with a maximum at 4.5 bohr and a height of 3.4 kcal/mol; see Fig. 7. The following vbL icon explains what is meant

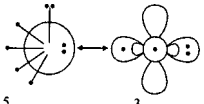

$\mathrm{Fe}(^5\mathrm{D};\mathrm{M}=\pm1)\ \mathrm{C}(^3\mathrm{P};\mathrm{M}=\mp1)$

Between 4.5 and 3.8 bohr an attractive interaction sets in due to a transfer of 0.25 e^- (at 4.2 bohr) to the $2p_z$ C orbital from the $4s^2$ of Fe, with a synchronous promotion of 0.40 e^- to the $4p_z$ of the Fe atom. At 3.8 bohr an avoided crossing occurs with the (not calculated) $^7\Sigma^+(2)$ state correlating to $\mathrm{Fe}(^5F;\mathrm{M}=0)+\mathrm{C}(^3P;\mathrm{M}=0)$. Notice the change of the M values from $(\pm1, \mp1)$ to (0, 0), resulting to a favorable for σ bonding electronic distribution. The Mulliken MRCI equilibrium atomic populations

$$4s^{0.86}4p_z^{0.21}3d_{z^2}^{0.89}3d_{xz}^{1.71}4p_x^{0.10}3d_{yz}^{1.71}4p_y^{0.10}3d_{x^2-y^2}^{1.01}3d_{xy}^{1.01}/$$
$$2s^{1.69}2p_z^{0.47}2p_x^{1.08}2p_y^{1.08}.$$

and the leading CFs at equilibrium dictate the following bonding picture

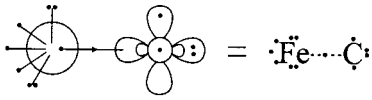

$\mathrm{Fe}(^5\mathrm{F};\mathrm{M}=0)\ \mathrm{C}(^3\mathrm{P};\mathrm{M}=0)\qquad {}^7\Sigma^+(1)$

suggesting a formal 1/2 σ bond. From Table II we read that at $r_e=1.766$ Å, $D_e=15.5$ kcal/mol with respect to the adiabatic products, or, diabatically, the internal bond strength is $15.5+\Delta E(^5F\leftarrow{}^5D)=39.7$ kcal/mol.

$$28{}^7\Sigma^-(2)(\sim|[0.56(1\sigma^2 2\sigma^2 3\sigma^2)+0.39(1\sigma^2 2\sigma^2 3\bar{\sigma}^1 4\sigma^1)$$
$$+0.27(1\sigma^2 2\sigma^2 3\sigma^1 4\bar{\sigma}^1)$$
$$-0.24(1\sigma^2 2\sigma^2 4\sigma^2)]1\pi_x^1 2\pi_x^1 1\pi_y^2 2\pi_y^1 1\delta_+^1 1\delta_-^1\rangle$$
$$+|1\sigma^2 2\sigma^2 3\sigma^1 4\sigma^1\{[0.30(1\pi_x^2 1\pi_y^1 2\pi_y^1+1\pi_x^1 2\pi_x^1 1\pi_y^2)$$
$$-0.20(2\pi_x^2 1\pi_y^1 2\pi_y^1+1\pi_x^1 2\pi_x^1 2\pi_y^2)]1\delta_+^1 1\delta_-^1$$
$$-0.27(1\pi_x^1 2\pi_x^1 1\pi_y^1 2\pi_y^1 1\delta_+^1 1\bar{\delta}_-^1)\}\rangle=|A_2\rangle,\mathrm{CASSCF}).$$

Notice that the leading configurations of the $13\,{}^7\Sigma^-(1)$ state described previously and the present one are the same. The asymptotic products are given by the product wave function $|^5D;\mathrm{M}=\pm1\rangle_{\mathrm{Fe}}\times|^3P;\mathrm{M}=\mp1\rangle_{\mathrm{C}}$, but the situation at equilibrium is not clear. An avoided crossing takes place at 4.5 bohr, Fig. 7, but we do not understand where the intervening $^7\Sigma^-(3)$ state correlates to, therefore, we do not know

the equilibrium atomic characters. Besides the numerical findings presented in Table II, nothing much can be said about the bonding of this state.

$30\,^7\Pi(3)$. This is a rather complicated state with two minima, a local (L) and a global (G) one (see Fig. 8), and five avoided crossings along its PEC. The L and G leading equilibrium CFs are

$$L:\ 0.67|1\sigma^2 2\sigma^2 3\sigma^1 4\sigma^1 1\pi_x^1(1\pi_y^1 2\pi_y^1 1\delta_+^1 1\delta_-^2 - 2\pi_x^1 1\pi_y^1 1\delta_+^2 1\delta_-^1)\rangle = |B_1\rangle, \text{CASSCF}$$

$$G:\ |1\sigma^2 2\sigma^1 3\sigma^1 4\sigma^1[0.58(1\pi_x^2) + 0.29(1\pi_x^1 2\overline{\pi}_x^1)]1\pi_y^2 2\pi_y^1 1\delta_-^1\rangle + |[0.36(1\sigma^2 2\sigma^1 3\sigma^2) + 0.35(1\sigma^2 2\sigma^2 3\sigma^1)]1\pi_x^1 2\pi_x^1 1\pi_y^2 2\pi_y^1 1\delta_+^1 1\delta_-^1\rangle + |1\sigma^2 2\sigma^1 3\sigma^1[0.21(1\pi_x^1 2\pi_x^1 1\pi_y^2 2\pi_y^1 1\delta_+^2 1\delta_-^1) - 0.20(1\pi_x^2 2\pi_x^1 1\pi_y^1 2\pi_y^1 1\delta_+^1 1\delta_-^2)]\rangle = |B_1\rangle, \text{MRCI}.$$

As the two atoms $\text{Fe}(^5D;\text{M}=0)+\text{C}(^3P;\text{M}=\pm1)$ approach from infinity, the first avoided crossing occurs at 5 bohr with a (not calculated) $^7\Pi(4)$ state correlating to $\text{Fe}(^5F;\text{M}=\pm1)+\text{C}(^3P;\text{M}=0)$, giving rise to a barrier of 6.8 kcal/mol (Fig. 8). A second avoided crossing occurs at 4.5 bohr with the $25\,^7\Pi(2)$ state (*vide supra*) correlating to $\text{Fe}(^5D;\text{M}=\pm2)+\text{C}(^3P;\text{M}=\mp1)$. At 4.13 bohr (=2.186 Å) the L minimum appears with a $D_e=8.74$ (8.8) kcal/mol at the MRCI(+Q) level. At this point the L Mulliken atomic densities are

$$4s^{1.07}4p_z^{0.42}3d_{z^2}^{1.06}3d_{xz}^{1.01}4p_x^{0.02}3d_{yz}^{1.01}4p_y^{0.02}3d_{x^2-y^2}^{1.50}3d_{xy}^{1.50}/ 2s^{1.85}2p_z^{1.51}2p_x^{0.51}2p_y^{0.51}.$$

The leading CFs and the above-mentioned distributions suggest the following bonding picture

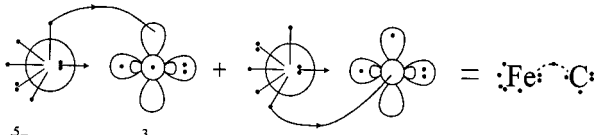

The bonding is comprised of a 1/2 π bond and a σ interaction due to a transfer of 0.35 e^- from the Fe $4s^2$ orbital to the $2p_z$ C orbital, and a promotion of 0.42 e^- to the Fe $4p_z$ orbital.

Leaving now the L minimum, a third avoided crossing takes place at 3.65 bohr with the (not calculated) $^7\Pi(4)$ state, which has suffered already at least a second avoided crossing (the first one was described previously), imparting, finally, a rather ionic character to the G minimum, $\text{Fe}^+(^6D;\text{M}=\pm1)+\text{C}^-(^4S)$. We hasten to add, however, that we are not certain about this conclusion because it is not corroborated by the electron transfer as deduced from the population analysis.

Two more avoided crossings are encountered at the repulsive part of the PEC: The fourth one at 3.4 bohr with the $25\,^7\Pi(2)$ state imparting a character of $\text{Fe}(^5F;\text{M}=\pm1)+\text{C}(^3P;\text{M}=0)$ to the PEC of this region, and finally a fifth one at 3.0 bohr, again with the $25\,^7\Pi(2)$ state (*vide infra*). The final character of the repulsive part of the $30\,^7\Pi(3)$ state is $\text{Fe}(^5D;\text{M}=\pm1)+\text{C}(^3P;\text{M}=0)$. (The L and G minima are practically degenerate at the MRCI level, but at the +Q level the energy of the G minimum drops by 6 mh with respect to the L.)

$$31\,^7\Phi(1)(\sim 0.67|1\sigma^2 2\sigma^2 3\sigma^1 4\sigma^1 1\pi_x^1(1\pi_y^1 2\pi_y^1 1\delta_+^1 1\delta_-^2 + 2\pi_x^1 1\pi_y^1 1\delta_+^2 1\delta_-^1)\rangle = |B_1\rangle, \text{CASSCF}).$$

This state correlates to $\text{Fe}(^5D;\text{M}=\pm2)+\text{C}(^3P;\text{M}=\pm1)$ and this character is transferred to the equilibrium geometry; see Fig. 8. It has the lowest binding energy of all other states presented in Table II, $D_e=8.2$ (8.4) kcal/mol at the MRCI(+Q) level, and the longer internuclear distance, $r_e=2.184$ Å. The similarity of the $31\,^7\Phi(1)$ with the above-described $30\,^7\Pi_L(3)$ state is striking: same configurations, bond distances, binding energies, and, of course, bonding nature. In the repulsive part of its PEC, the $31\,^7\Phi(1)$ state suffers an avoided crossing at about 3.5 bohr with a (not calculated) $^7\Phi(2)$ state, which rather correlates to $\text{Fe}(^5F;\text{M}=\pm3)+\text{C}(^3P;\text{M}=0)$.

D. Singlets: $1\,^1\Delta(1)$, $11\,^1\Pi(1)$, $14\,^1\Gamma(1)$, $19\,^1\Sigma^+(1)$, $21\,^1\Sigma^-(1)$, $32\,^1\Delta(2)$, $35\,^1\text{H}(1)$, $36\,^1\Pi(2)$, $37\,^1\Phi(1)$, $38\,^1\Phi(2)$, $39\,^1\Pi(3)$, and $40\,^1\Delta(3)$

$$1\,^1\Delta(1)(\sim|[0.77(1\sigma^2 2\sigma^2 3\sigma^1)+0.22(1\sigma^2 2\sigma^2 4\sigma^1)] \times 1\pi_x^2 1\pi_y^2 1\overline{\delta}_+^1 1\delta_-^2\rangle = |A_1\rangle, \text{CASSCF}).$$

As was previously mentioned [state $2\,^3\Sigma^-(1)$] our results indicate that the $^1\Delta(1)$ is the first excited state being 9.8(9.4), 9.5(9.1), 9.7(9.5) kcal/mol above the *X* state in the sequence of MRCI(+Q), MRCI/large(+Q), C-MRCI/large(+Q) calculations, respectively (Table II). Notice that the $T_e(^1\Delta\leftarrow X)$ value remains, practically, method independent. The difference from the *X* state is a spin flip of the δ_+ orbital, $\overline{\delta}_+^1$ instead of δ_+^1 (or $\overline{\delta}_-^1$ instead of δ_-^1 in A_2 symmetry). It traces its lineage to $\text{Fe}(^3F;\text{M}=\pm2)+\text{C}(^3P;\text{M}=0)$, while the asymptotic atomic characters are transferred to equilibrium (Fig. 9). The CASSCF atomic populations

$$4s^{0.91}4p_z^{0.20}3d_{z^2}^{1.27}3d_{xz}^{1.16}4p_x^{0.03}3d_{yz}^{1.16}4p_y^{0.03}3d_{x^2-y^2}^{1.00}3d_{xy}^{1.99}/ 2s^{1.79}2p_z^{0.81}2p_x^{0.79}2p_y^{0.79},$$

coupled with the leading CFs indicate the formation of one σ and two π bonds. The corresponding vbL icon is clearly (A_2 symmetry) the following

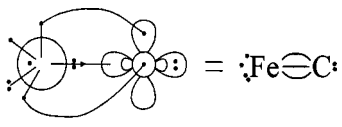

Through the π frame about 0.4 e^- migrate from the C to the metal, and through the σ skeleton 0.60 e^- are transferred from the $(3d_z2)^{2.0}$ of the metal to the empty $2p_z$ C orbital giving rise to the σ bond. The bonding is identical to that of

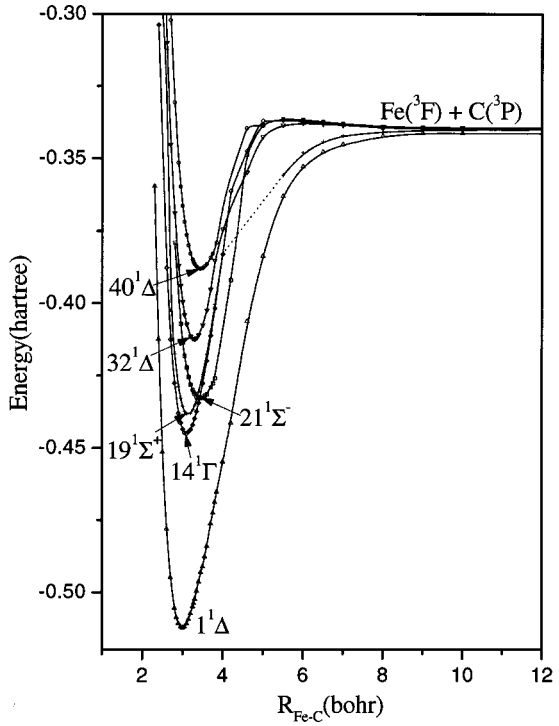

FIG. 9. MRCI potential-energy curves of the singlets $1\,^1\Delta(1)$, $14\,^1\Gamma(1)$, $19\,^1\Sigma^+(1)$, $21\,^1\Sigma^-(1)$, $32\,^1\Delta(2)$, and $40\,^1\Delta(3)$ of the FeC molecule. Dotted line is referred to that part of the $19\,^1\Sigma^+(1)$ state that has not been calculated.

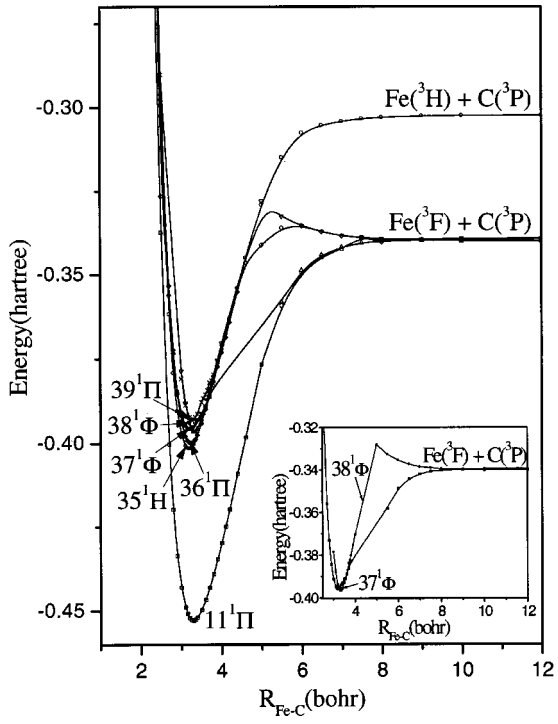

FIG. 10. MRCI potential-energy curves of the singlets $11\,^1\Pi(1)$, $35\,^1\mathrm{H}(1)$, $36\,^1\Pi(2)$, $37\,^1\Phi(1)$, $38\,^1\Phi(2)$, and $39\,^1\Pi(3)$. Inset: MRCI potential-energy curves of $37\,^1\Phi(1)$ and $38\,^1\Phi(2)$ states.

the $X\,^3\Delta$ state (*vide supra*), and this is reflected to, practically, the same bond length between the two states and rather similar bond strengths (Table II). As we can see from Table II, the r_e, ω_e, and $\omega_e x_e$ values are in fair agreement with recent experimental results obtained by Aiuchi *et al.* by dispersed fluorescence spectroscopy.[14] The same workers determined the transition, first excited state$\leftarrow X\,^3\Delta$, $T_0 = 3460\ \mathrm{cm}^{-1}(=9.893\ \mathrm{kcal/mol})$ or $T_e=(T_0+\Delta\omega_e/2) = 9.786\ \mathrm{kcal/mol}$, suggesting also that the first excited state is of $^5\Pi$ symmetry. Our results clearly indicate that the first excited state is of $^1\Delta$ symmetry; the same conclusion was reached by SG[6] and Hirano *et al.*;[7] see Table II. Finally, we would like to mention that the $^1\Delta$ state has the largest binding energy, $D_e=107.4$ (109) kcal/mol at the MRCI(+Q) level, and the smallest internuclear distance, $r_e=1.585$ Å of all states studied. The corresponding MRCI/large(+Q) and C-MRCI/large(+Q) values are 110.0(112), 111.0(114) kcal/mol, and 1.575, 1.566 Å, respectively.

$$11\,^1\Pi(1)(\sim 0.56|1\sigma^2 2\sigma^2 3\bar{\sigma}^1 1\pi_x^2 1\pi_y^2 2\pi_y^1 1\delta_+^1 1\bar{\delta}_-^1\rangle$$
$$+0.32|1\sigma^2 2\sigma^2 3\sigma^1 1\pi_x^2 1\pi_y^2 2\bar{\pi}_y^1 1\delta_+^1 1\bar{\delta}_-^1\rangle$$
$$+0.21|1\sigma^2 2\sigma^1 3\sigma^2 1\pi_x^2 1\pi_y^2 2\pi_y^1 1\bar{\delta}_+^1 1\bar{\delta}_-^1\rangle$$
$$=|B_1\rangle,\mathrm{MRCI}).$$

Figure 10 presents the PEC of the $^1\Pi(1)$ state correlating to $\mathrm{Fe}(^3F;\mathrm{M}=\pm1)+\mathrm{C}(^3P;\mathrm{M}=0)$; this character is maintained at the equilibrium, $r_e=1.741$ (1.717) Å at the MRCI(+Q) level, Table II. At this geometry the MRCI Mulliken densities are

$$4s^{0.95}4p_z^{0.24}3d_{z^2}^{1.23}3d_{xz}^{1.20}4p_x^{0.04}3d_{yz}^{1.92}4p_y^{0.08}3d_{x^2-y^2}^{1.01}3d_{xy}^{1.01}/$$
$$2s^{1.71}2p_z^{0.80}2p_x^{0.74}2p_y^{0.96},$$

which, in conjunction with the main CFs and the symmetry of the *in situ* atoms, support the following bonding picture (B_1 symmetry)

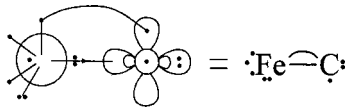

The two atoms are held together by a π and a σ bond, the latter formed by a transfer of 0.50 e^- from the $\mathrm{Fe}(3d_z2)^2$ orbital to the (empty) $2p_z$ C orbital, with the synchronous promotion of 0.24 e^- to the $4p_z$ (Fe) orbital; via the π frame, 0.25 e^- migrate from the C to the Fe atom. Our numerical results are in qualitative agreement with the corresponding results of SG[6] (Table II).

$14\,^1\Gamma(1)$. The PEC presented in Fig. 9 shows that the fragments at infinity are $\mathrm{Fe}(^3F;\mathrm{M}=\pm3)+\mathrm{C}(^3P;\mathrm{M}=\pm1)$. It is of interest to give the CASSCF CFs in both symmetries A_1 and A_2 "compatible" with the Γ symmetry.

$$14\,^1\Gamma(1)/A_1\sim 0.59|1\sigma^2 2\sigma^2 3\sigma^2 1\pi_x^2 1\pi_y^2(1\delta_+^2+1\delta_-^2)\rangle$$
$$14\,^1\Gamma(1)/A_2\sim 0.83|1\sigma^2 2\sigma^2 3\sigma^2 1\pi_x^2 1\pi_y^2 1\delta_+^1 1\bar{\delta}_-^1)\rangle.$$

Of course, a true Γ state is a linear combination of the A_1 and A_2 components, $2(0.59)^2\approx 0.83^2$.

Moving from infinity towards equilibrium, an avoided crossing occurs around 4.2 bohr with the $^1\Gamma(2)$ state possi-

bly correlating to $Fe(^3H;M=\pm 3 \text{or} \mp 5)+C(^3P;M=\pm 1)$. This atomic character is imparted to equilibrium with the following Mulliken CASSCF distributions,

$$4s^{1.20}4p_z^{0.23}3d_{z^2}^{1.62}3d_{xz}^{1.31}4p_x^{0.03}3d_{yz}^{1.31}4p_y^{0.03}3d_{x^2-y^2}^{1.01}3d_{xy}^{1.01}/$$
$$2s^{1.81}2p_z^{1.08}2p_x^{0.66}2p_y^{0.66}.$$

In A_2 symmetry the bonding can be visualized by the icon

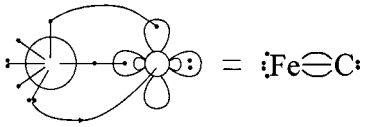

$Fe(^3H;\ M=\pm 3,\ \text{or}\ \mp 5)\ C(^3P;\ M=\pm 1) \quad {}^1\Gamma(1)$

Through the π frame 0.3 e^- are transferred from Fe to C, while, clearly, two π bonds are formed. The σ bond is formed due to the $2p_z(C)+(4s4p_z3d_{z^2})^{3.0}$ (Fe) interaction; less than 0.1 e^- seems to be transferred from C to Fe through the σ frame. A $D_e=66.1$ kcal/mol (MRCI) is predicted with respect to $Fe(^3F)+C(^3P)$, however, with respect to the diabatic products $Fe(^3H)+C(^3P)$, the internal bond strength is $66.1+\Delta E(^3H\leftarrow{}^3F)^{13}=86.6$ kcal/mol.

$$19^1\Sigma^+(1) \quad (\sim 0.56|1\sigma^2 2\sigma^2 3\sigma^2 1\pi_x^2 1\pi_y^2(1\delta_+^2+1\delta_-^2)\rangle$$
$$-0.22|1\sigma^2 2\sigma^1 3\bar{\sigma}^1 4\sigma^2 1\pi_x^2 1\pi_y^2 1\delta_-^2\rangle=|A_1\rangle,\text{CASSCF}).$$

At infinity this state is represented by the product wave function, $|^3F;M=0\rangle_{Fe}\times|^3P;M=0\rangle_C$; see Fig. 9. Severe convergence problems, probably caused by an avoided crossing, prevented us from calculating the PEC's part between 5.5 and 4.0 bohr. The assumed avoided crossing between 5.0 and 4.0 bohr is due to a (not calculated) $^1\Sigma^+(2)$ state correlating rather to $Fe(^3H \text{ or } ^3P;M=\pm 1)+C(^3P;M=\mp 1)$, thusly transferring this character to the *in situ* equilibrium atoms. The binding mode is very similar to that of the previously discussed $^1\Gamma(1)$ state as is also reflected in the D_e and r_e values (Table II)

$$21^1\Sigma^-(1)(\sim|[0.51(1\sigma^2 2\sigma^2 3\sigma^1 4\sigma^1)$$
$$-0.24(1\sigma^2 2\sigma^1 3\sigma^2 4\sigma^1)]1\pi_x^2 1\pi_y^2 1\delta_+^1 1\bar{\delta}_-^1\rangle$$
$$-0.29|1\sigma^2 2\sigma^2 3\sigma^1 4\bar{\sigma}^1 1\pi_x^2 1\pi_y^2 1\delta_+^1 1\bar{\delta}_-^1\rangle$$
$$-|1\sigma^2 2\sigma^2 3\sigma^1 4\sigma^1[0.17(2\pi_x^2 1\pi_y^2+1\pi_x^2 2\pi_y^2)$$
$$+0.16(1\bar{\pi}_x^1 2\pi_x^1 1\pi_y^2+1\pi_x^2 1\bar{\pi}_y^1 2\pi_y^1)]1\bar{\delta}_+^1 1\bar{\delta}_-^1\rangle$$
$$=|A_2\rangle,\text{MRCI}).$$

The *in situ* atomic characters at equilibrium are the same with the asymptotic fragments, $Fe(^3F;M=\pm 1)+C(^3P;M=\mp 1)$; see Fig. 9. The MRCI atomic distributions at $r_e=1.820$ Å are

$$4s^{0.98}4p_z^{0.40}3d_{z^2}^{1.88}3d_{xz}^{1.17}4p_x^{0.05}3d_{yz}^{1.17}4p_y^{0.05}3d_{x^2-y^2}^{1.00}3d_{xy}^{1.00}/$$
$$2s^{1.70}2p_z^{0.96}2p_x^{0.77}2p_y^{0.77},$$

consistent with the formation of two π bonds and the transfer of 0.54 e^- via the π frame from Fe to the C atom. As usual the σ interaction is not so clear; we can only say that 0.24 e^- migrate back from the C to the Fe atom through the σ frame, populating the $4p_z$ orbital of the latter: 0.40 $e^-\approx 0.24+0.12$ (from $3d_z2$) $+0.02$ (from $4s$). In other words, the σ interaction is caused by promoting 0.40 e^- to the $4p_z$ (empty at infinity) Fe orbital. However, we would like to remark that the PEC's shape (Fig. 9) is not very "natural," reminiscent of an harmonic oscillator potential. It should be mentioned that we were unable to converge CASSCF energy points in the region 3.9 to 4.4 bohr for this state.

$32\,^1\Delta(2)$, $40\,^1\Delta(3)$. The states $^1\Delta(2)$ and $^1\Delta(3)$ correlate to $Fe(^3F;M=\mp 3,\pm 1)+C(^3P;M=\pm 1)$, respectively (Fig. 9). Their main equilibrium CASSCF ($^1\Delta(2)$) and MRCI ($^1\Delta(3)$) CFs are

$$32^1\Delta(2):\sim|[0.54(1\sigma^2 2\sigma^1 3\sigma^2)+0.41(1\sigma^2 2\sigma^2 3\sigma^1)$$
$$-0.19(1\sigma^2 2\sigma^1 4\sigma^2)]1\pi_x^2 1\pi_y^2 1\delta_+^2 1\bar{\delta}_-^1\rangle$$
$$-0.20|1\sigma^2 2\sigma^1 3\sigma^2(1\pi_x^2 2\pi_y^2$$
$$+2\pi_x^2 1\pi_y^2)1\delta_+^2 1\bar{\delta}_-^1\rangle=|A_2\rangle$$

$$40^1\Delta(3):\sim|1\sigma^2 2\sigma^2 3\sigma^1[0.37(1\bar{\pi}_x^1 2\pi_x^1 1\pi_y^2$$
$$+1\pi_x^2 1\bar{\pi}_y^1 2\pi_y^1)+0.25(1\pi_x^1 2\bar{\pi}_x^1 1\pi_y^2$$
$$+1\pi_x^2 1\pi_y^1 2\bar{\pi}_y^1)]1\delta_+^2 1\bar{\delta}_-^1\rangle-|1\sigma^2 2\sigma^1 3\sigma^2$$
$$\times[0.26(1\pi_x^2 1\pi_y^2)-0.20(1\bar{\pi}_x^1 2\pi_x^1 1\pi_y^2+$$
$$+1\pi_x^2 1\bar{\pi}_y^1 2\pi_y^1)]1\delta_+^2 1\bar{\delta}_-^1\rangle=|A_2\rangle.$$

At 3.8 bohr an avoided crossing between these two Δ states causes the exchange of the M values of the metal. Their equilibrium CASSCF populations are as follows for the $^1\Delta(2)$ and $^1\Delta(3)$ states (populations of $^1\Delta(3)$ in parentheses)

$$4s^{1.03(0.94)}4p_z^{0.24(0.29)}3d_{z^2}^{1.02(1.10)}3d_{xz}^{1.19(1.15)}4p_x^{0.03(0.03)}$$
$$3d_{yz}^{1.19(1.15)}4p_y^{0.03(0.03)}3d_{x^2-y^2}^{1.94(1.93)}3d_{xy}^{1.00(0.95)}/2s^{1.74(1.80)}$$
$$2p_z^{0.98(0.86)}2p_x^{0.78(0.87)}2p_y^{0.78(0.87)}.$$

Without doubt, in both states, the bonding consists of two π and one σ bonds as shown in the vbL diagram (A_2 components),

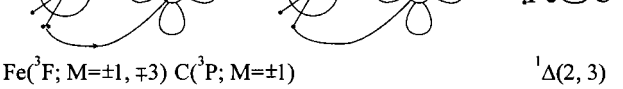

$Fe(^3F;\ M=\pm 1,\mp 3)\ C(^3P;\ M=\pm 1) \qquad {}^1\Delta(2,3)$

The net electron transfer from Fe to C is 0.30 and 0.40 e^- for the $^1\Delta(2)$ and $^1\Delta(3)$ states, respectively.

$$35\,^1\text{H}(1)(\sim 0.47|1\sigma^2 2\sigma^2 3\sigma^1 1\pi_x^2 1\pi_y^2 2\bar{\pi}_y^1 1\delta_+^1 1\bar{\delta}_-^1\rangle$$
$$+0.38|1\sigma^2 2\sigma^2 3\sigma^1 1\pi_x^2 2\bar{\pi}_x^1 1\pi_y^2(1\delta_+^2-1\delta_-^2)\rangle$$
$$-0.27|1\sigma^2 2\sigma^2 3\bar{\sigma}^1 1\pi_x^2 1\pi_y^2 2\pi_y^1 1\delta_+^1 1\bar{\delta}_-^1\rangle,\text{CASSCF}).$$

This is the highest $\Lambda(=5)$ state of the present report; it

correlates to Fe(^3H;M$=\pm5$)+C(^3P;M$=0$), Fig. 10, and the last state formally bound with respect to the ground-state products by just 0.2 kcal/mol, but strongly bound ($D_e=62.4$ kcal/mol at the MRCI level) with respect to the asymptotic products. Although we were unable to locate any avoided crossings, we cannot exclude an interaction with an ^{1}H(2) state originating from Fe($b\,^3H$;M$=\pm5$)+C(^3P;M$=0$); the Fe($b\,^3H$) state is 19.3 kcal/mol above the Fe($a\,^3H$). The equilibrium CASSCF atomic densities

$$4s^{0.89}4p_z^{0.30}3d_{z^2}^{1.16}3d_{xz}^{1.58}4p_x^{0.04}3d_{yz}^{1.58}4p_y^{0.04}3d_{x^2-y^2}^{1.00}3d_{xy}^{1.00}/$$
$$2s^{1.80}2p_z^{0.83}2p_x^{0.87}2p_y^{0.87},$$

suggest the following bonding icon (B_1 component)

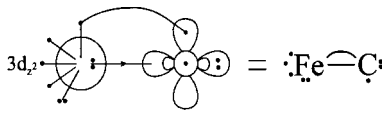

Through the π interaction 0.26 e$^-$ move from the C to the Fe atom. The σ bond seems to be caused, given the reservations expressed before concerning the interaction with an ^{1}H(2) molecular state, by the transfer of 0.63 e$^-$ from the $4s^2$ Fe orbital to the $2p_z$ (empty at infinity) C orbital, and the promotion of 0.30+0.16 e$^-$ to the $4p_z$ and $3d_z2$ Fe orbitals, respectively. Alternatively, from the hybrid $(4s4p_z3d_z2)^{3.0}$ on the Fe center, 0.63 e$^-$ diffuse to the $2p_z$ C orbital.

$$36\,^1\Pi(2)(\sim|1\sigma^2 2\sigma^2 3\sigma^1\{1\pi_x^2 2\bar{\pi}_x^1 1\pi_y^2[0.42(1\delta_+^2)$$
$$+0.41(1\delta_-^2)]-[0.40(1\bar{\pi}_x^1 1\pi_y^2)+0.24(2\bar{\pi}_x^1,1\pi_y^2)$$
$$+0.17(1\bar{\pi}_x^1 1\pi_y^1 2\bar{\pi}_y^1 x)]1\delta_+^2 1\bar{\delta}_-^1\}\rangle=|B_1\rangle,\text{MRCI},$$

$$39\,^1\Pi(3)(\sim 0.44|1\sigma^2 2\sigma^2 3\sigma^2(1\bar{\pi}_x^1 1\pi_y^2 1\delta_+^1 1\delta_-^2$$
$$-1\pi_x^2 1\pi_y^1 1\delta_+^2 1\bar{\delta}_-^1)\rangle-0.29|1\sigma^2 2\sigma^2 3\sigma^1 1\pi_x^2 2\bar{\pi}_x^1$$
$$\times 1\pi_y^2(1\delta_+^2+1\delta_-^2)\rangle=|B_1\rangle,\text{MRCI}).$$

The energy difference between the above $^1\Pi$ states is 4.4 (3.6) kcal/mol at the MRCI(+Q) level (Table II). They correlate to Fe(^3F;M$=0,\pm2$)+C(^3P;M$=\mp1$), states 36 and 39, respectively. For both states nothing much can be said about the bonding. An interaction between them occurs within 3.8–4.0 bohr, while the equilibrium character of the *in situ* atoms of the $^1\Pi(2)$ state seems to be the same with the asymptotic fragments; we are not sure for the equilibrium atomic character of the $^1\Pi(3)$ state. Also, for the latter, we were unable to construct the PEC's region between 4.2 to 9 bohr due to severe technical problems (Fig. 10). Given our reservations, we claim that the bonding for both states consists of a single π bond.

$$37\,^1\Phi_G(1)(\sim|1\sigma^2 2\sigma^2 3\sigma^2[0.45(1\bar{\pi}_x^1 1\pi_y^2 1\delta_+^1 1\delta_-^2$$
$$+1\pi_x^2 1\pi_y^1 1\delta_+^2 1\bar{\delta}_-^1)+0.16(1\pi_x^2 2\pi_y^1 1\delta_+^2 1\bar{\delta}_-^1$$
$$+2\bar{\pi}_x^1 1\pi_y^2 1\delta_+^1 1\delta_-^2-1\pi_x^2 1\pi_y^2 2\pi_y^1 1\bar{\delta}_-^1)]\rangle=|B_1\rangle,\text{MRCI}$$

$$38\,^1\Phi(2)(\sim|1\sigma^2 2\sigma^2 3\sigma^1 1\pi_x^2 1\pi_y^2[0.47(2\bar{\pi}_y^1 1\delta_+^1 1\bar{\delta}_-^1)$$
$$-0.27(2\pi_y^1 1\bar{\delta}_+^1 1\bar{\delta}_-^1)]\rangle$$
$$-0.39|1\sigma^2 2\sigma^2 3\sigma^2 1\pi_x^2 2\bar{\pi}_x^1 1\pi_y^2 1\delta_+^1\rangle$$
$$+0.38|1\sigma^2 2\sigma^2 1\pi_x^2 2\bar{\pi}_x^1 1\pi_y^2 1\delta_+^1 1\delta_-^2\rangle=|B_1\rangle,\text{MRCI}).$$

The two states, 37 and 38, correlate to Fe(^3F;M$=\pm3$, ±2)+C(^3P;M$=0,\pm1$), respectively, with their corresponding PECs shown in Fig. 10 (see also inset). As we move towards the equilibrium and around 5 bohr, the $^1\Phi(2)$ state suffers an avoided crossing with a (not calculated) $^1\Phi(3)$ state correlating to Fe(^3H;M$=\pm4$or∓2)+C(^3P;M$=\mp1$), and at 3.65 and 3.25 bohr two additional avoided crossings occur between the $^1\Phi(1)$ and $^1\Phi(2)$ states. As a result the $^1\Phi(1)$ presents a global minimum at r_e(G)$=1.756$ Å ($=3.32$ bohr) with atomic *in situ* characters of Fe(^3H;M$=\pm4$or∓2)+C(^3P;M$=\mp1$) and a local minimum at r_e(L)$=1.745$ Å($=3.30$ bohr) with *in situ* atomic characters of the asymptotic fragments. The minimum of the $^1\Phi(2)$ appears at 3.25 bohr, on top of the second avoided crossing between the $\Phi(1)$ and $\Phi(2)$ states; see Fig. 10.

Of course, for the $^1\Phi(2)$ state, spectroscopic constants lack of meaning and only formal D_e and r_e values are given in Table II. Also, the type of leading CFs involved in the MRCI expansion of the $^1\Phi(1)$ state do not allow any clear description of the bonding in the global minimum. As a matter of fact conventional bonding pictures break down for such states, so there is no meaning in discussing the bonding mechanism.

V. SYNOPSIS AND REMARKS

For the FeC diatomic, a 12 active electron system, we have performed multireference variational calculations, specifically, CASSCF+1+2=MRCI, with a [$7s6p4d3f/_{\text{Fe}}$cc-pVTZ/$_{\text{C}}$] basis set. For three out of 41 states examined, i.e., the ground FeC($^3\Delta$), and the first two excited states ($^1\Delta$ and $^3\Sigma^-$), calculations were also done at the larger basis set [$7s6p4d3f2g/_{\text{Fe}}$cc-pVQZ/$_{\text{C}}$] (MRCI/large). In addition, for these three states we examined the results of core correlation effects by including the Fe $3s^23p^6$ electrons at the MRCI level (C-MRCI/large). For reasons of comparison the $X\,^3\Delta$ state was also examined at the CCSD(T)/small level of theory.

For all states we report total energies, equilibrium bond distances, dissociation energies, dipole moments, and the most common spectroscopic constants (ω_e, $\omega_e x_e$, α_e, and $\bar{D}_e$) obtained by a Dunham analysis. Full potential-energy curves were also constructed for almost all states with the purpose of following the evolution of the atomic states along the reaction coordinate. A synopsis of our findings and conclusions follows.

(1) The FeC molecule is a genuine multireference system, therefore it is close to impossible to be tackled by any single reference-type method. For many of the examined states the largest variational CASSCF (or MRCI) expansion coefficients do not exceed the value of 0.4. Also, the existing DFT data seems to be in stark dis-

agreement with corresponding experimental results or quality *ab initio* values. The same general disagreement between DFT and high level *ab initio* results was also recorded for the diatomic carbides ScC[2] and TiC.[25]

(2) For the ground state ($X\,^3\Delta$) and at the highest level of our calculations (C-MRCI/large), we predict a binding energy $D_e = 86.7$ kcal/mol. By correcting this value for BSSE and scalar relativistic effects,[6] we obtain $D_e = 84.3$ kcal/mol. These values should be contrasted with two experimental values 91.2 ± 7 kcal/mol (upper limit),[11] and 81.7 ± 4.6 kcal/mol,[15] or with their average of 86.5 ± 5.8 kcal/mol.

(3) The recently assigned by dispersed fluorescence spectroscopy $^5\Pi$ state of FeC, ~10 kcal/mol above the X state, certainly has a different symmetry. Two states compete for that energy position in our calculations, a $^1\Delta$ and a $^3\Sigma^-$. Our final results at the C-MRCI/large level suggest, with some confidence, that the $^1\Delta$ is the first excited state 9.7 kcal/mol above the X state. At the same level of theory the corresponding splitting for the $^3\Sigma^-$ state is 14.1 kcal/mol; however, the Davidson correction brings those numbers to 9.5 and 10.8 kcal/mol, respectively, or that $\Delta E\,(^3\Sigma^- - {}^1\Delta) = 1.3$ kcal/mol.

(4) With the exception of $18\,^3\Phi(1)$ state all our results are in good agreement with existing experimental data. For the $^3\Phi(1)$ state all our calculated parameters are in disagreement with experimental values. Our results suggest that, perhaps, this experimentally assigned $^3\Phi$ state is of $^3\Pi$ symmetry, specifically the $8\,^3\Pi(2)$ state.

(5) All calculated states are bound with respect to their asymptotic products; with respect to ground state fragments, 35 states are bound, the last one being the ^{1}H(1) state. The $^1\Delta(1)$ state has the largest binding energy (with respect to its asymptotic products), and the shortest bond length of all calculated states, namely, $D_e = 111.0$ kcal/mol at $r_e = 1.566$ Å at the C-MRCI/large level.

(6) In all states a net charge transfer is observed from Fe to C ranging from about 0.50 e^- to 0.25 e^- at the CASSCF level. At the MRCI this Fe→C electron transfer is diminished on the average by 0.1 e^-.

(7) All our computed states correlate to the ground-state carbon atom, C(^3P;M=0,±1). In all cases where the *in situ* equilibrium C atom has the M=0 character, i.e., two electrons distributed ''perpendicularly'' to the internuclear axis, a strong transfer of electrons is observed from Fe to C along the σ frame, thus, resulting in a very strong σ bond and rather high D_e values; see, for instance, the $X\,^3\Delta$ and $1\,^1\Delta(1)$ states. In cases where the *in situ* C finds itself in a M=±1 state, the σ interaction is turned off or it is very weak, and the charge transfer from Fe to C is forced to occur mainly through the π frame.

(8) In the X and the first (1) excited state, as well as in the 2, 7, 14, 19, 29, 32, 33, and 40 states, the two atoms are held by a triple bond.

(9) For all states and for obvious reasons, the $d_{x^2-y^2}(\delta_+)$ and $d_{xy}(\delta_-)$ electrons remain strictly localized on the Fe atom; therefore, they do not play any significant role in the binding process.

(10) For many states of the FeC system the entangling of states of the same symmetry creates severe technical difficulties, sometimes unsolved, particularly if one wishes to compute complete potential-energy curves. However, in most cases complete PECs are necessary because the bonding depends on the detailed history of the atoms from infinity to equilibrium.

(11) The T_e's of the following pairs or groups differ by about 1 mhartree and obviously the real ordering is possibly different, $\{8\,^3\Pi(2), 9\,^7\Delta(1)\}$, $\{10\,^7\Pi(1), 11\,^1\Pi(1)\}$, $\{11\,^1\Pi(1), 12\,^5\Sigma^-(1)\}$, $\{17\,^5\Pi(2), 18\,^3\Phi(1)\}$, $\{18\,^3\Phi(1), 19\,^1\Sigma^+(1)\}$, $\{23\,^5\Sigma^+(1), 24\,^5\Pi(3)\}$, $\{24\,^5\Pi(3), 25\,^7\Pi(2)\}$, $\{25\,^7\Pi(2), 26\,^5\Phi(1)\}$, $\{26\,^5\Phi(1), 27\,^7\Sigma^+(1)\}$, $\{30\,^7\Pi(3), 31\,^7\Phi(1)\}$ and $\{37\,^1\Phi(1), 38\,^1\Phi(2)\}$. The ordering is reversed by adding the zero-point energy correction $\Delta\omega_e/2$ for the pairs $\{8\,^3\Pi(2), 9\,^7\Delta(1)\}$, $\{26\,^5\Phi(1), 27\,^7\Sigma^+(1)\}$ and $\{30\,^7\Pi(3), 31\,^7\Phi(1)\}$ by 0.2, 0.1, and 0.1 kcal/mol, respectively; the two states $37\,^1\Phi(1)$ and $38\,^1\Phi(2)$ cannot be distinguished, the second state being lower than the zero-point energy of the first one. Last, by applying the Davidson +Q correction, the ordering is reversed for the groups $\{11\,^1\Pi(1), 12\,^5\Sigma^-(1), 10\,^7\Pi(1)\}$, $\{14\,^1\Gamma(1), 13\,^7\Sigma^-(1)\}$, $\{16\,^3\Sigma^-(2), 18\,^3\Phi(1), 19\,^1\Sigma^+(1), 17\,^5\Pi(2), 15\,^5\Delta(2)\}$, $\{27\,^7\Sigma^+(1), 26\,^5\Phi(1), 23\,^5\Sigma^+(1), 24\,^5\Pi(3), 22\,^7\Delta(2), 25\,^7\Pi(2)\}$, $\{32\,^1\Delta(2), 31\,^7\Phi(1)\}$, and $\{36\,^1\Pi(2), 35\,^1H(1)\}$.

[1] I. S. K. Kerkines and A. Mavridis, J. Phys. Chem. A **104**, 11777 (2000).
[2] A. Kalemos, A. Mavridis, and J. F. Harrison, J. Phys. Chem. A **105**, 755 (2001).
[3] R. S. DaBell, R. G. Meyer, and M. D. Morse, J. Chem. Phys. **114**, 2938 (2001).
[4] See for instance, J. F. Harrison, Chem. Rev. **100**, 679 (2000), and references therein.
[5] B. K. Nash, B. K. Rao, and P. Jena, J. Chem. Phys. **105**, 11020 (1996).
[6] I. Shim and K. A. Gingerich, Eur. Phys. J. D **7**, 163 (1999).
[7] S. S. Itono, T. Taketsugu, T. Hirano, and U. Nagashima, J. Chem. Phys. **115**, 11213 (2001).
[8] R. M. Sosa, P. Gardiol, and G. Beltrame, Int. J. Quantum Chem. **65**, 919 (1997).
[9] W. J. Balfour, J. Cao, C. V. V. Prasad, and C. X. W. Qian, J. Chem. Phys. **103**, 4046 (1995).
[10] N. D. Allen, T. C. Pesch, and L. M. Ziurys, Astrophys. J. Lett. **472**, L57 (1996).
[11] D. J. Brugh and M. D. Morse, J. Chem. Phys. **107**, 9772 (1997).
[12] R. L. Hettich and B. S. Freiser, J. Am. Chem. Soc. **108**, 2537 (1986).
[13] C. E. Moore, *Atomic Energy Levels*, NSRDS-NBS Circular No. 35 (Washington, DC 1971).
[14] K. Aiuchi, K. Tsuji, and K. Shibuya, Chem. Phys. Lett. **309**, 229 (1999).
[15] C. Angeli, G. Berthier, C. Rolando, M. Sablier, C. Alcaraz, and O. Dutuit, J. Phys. Chem. A **101**, 7907 (1997).
[16] J. W.-H. Leung, W. S. Tam, Q. Rin, and A. S.-C. Cheung, Chem. Phys. Lett. **343**, 64 (2001).
[17] A. Kalemos and A. Mavridis, Adv. Quantum Chem. **32**, 69 (1998); A. Kalemos and A. Mavridis, J. Phys. Chem. A **102**, 5982 (1998); A. Kalemos and A. Mavridis, *ibid.* **103**, 3336 (1999); A. Kalemos and A. Mavridis, J. Chem. Phys. **113**, 2270 (2000).
[18] C. W. Bauschlicher, Jr., Theor. Chim. Acta **92**, 183 (1995).
[19] T. H. Dunning, Jr., J. Chem. Phys. **90**, 1007 (1989).
[20] H.-J. Werner and P. J. Knowles, J. Chem. Phys. **89**, 5803 (1988); P. J. Knowles and H.-J. Werner, Chem. Phys. Lett. **145**, 514 (1988); H.-J.

Werner and E. A. Reinsch, J. Chem. Phys. **76**, 3144 (1982); H.-J. Werner, Adv. Chem. Phys. **LXIX**, 1 (1987).
[21] K. Docken, and J. Hinze, J. Chem. Phys. **57**, 4928 (1972); H.-J. Werner and W. Meyer, J. Chem. Phys. **74**, 5794 (1981).
[22] S. F. Boys and F. Bernardi, Mol. Phys. **19**, 553 (1970).
[23] S. R. Langhoff and E. R. Davidson, Int. J. Quantum Chem. **8**, 61 (1974); M. R. A. Blomberg and P. E. M. Sieghbahm, J. Chem. Phys. **78**, 5682 (1983).
[24] MOLPRO 2000 is a package of *ab initio* programs written by H.-J. Werner and P. J. Knowles, with contributions by R. D. Amos, A. Bernhardsson, A. Berning *et al.*
[25] A. Kalemos and A. Mavridis, J. Phys. Chem. A. (accepted).